

NPS72-86-004CR

NAVAL POSTGRADUATE SCHOOL

Monterey, California



CONTRACTOR REPORT

IMPULSIVE LOADING FROM A BARE
EXPLOSIVE CHARGE IN SPACE

by

Joseph Falcovitz

December 1986

Approved for public release; distribution unlimited.

Prepared for: Strategic Defense Initiative Office
The Pentagon
Washington, DC 20301-7100

FedDocs
D 208.14/2
NPS-72-86-004CR

Feb 1985

U 208.14/2:

NP-12-86-004CP

DUDLEY KNOX LIBRARY
NAVAL POSTGRADUATE SCHOOL
MONTEREY, CALIFORNIA 93943-5002

NAVAL POSTGRADUATE SCHOOL
Monterey, California

RADM R. C. Austin
Superintendent

D. A. Schradly
Provost

The work reported herein was performed for the Naval Postgraduate School by Dr. Joseph Falcovitz under contract N00228-87-C-3046. The work presented in this report is in support of "Rarefied Gas Dynamics of Laser Exhaust Plume" sponsored by the Strategic Defense Initiative Office/Directed Energy Office. This is a partial report for that contract. The work provides information on impulsive loading of and damage to space targets due to an explosion of a bare charge. The project at the Naval Postgraduate School is under the cognizance of Distinguished Professor A. E. Fuhs who is principal investigator.

Reproduction of all or part of this report is authorized.

Prepared by:

REPORT DOCUMENTATION PAGE

DUDLEY KNOX LIBRARY
NAVAL POSTGRADUATE SCHOOL
MONTEREY CA 93943-5007

1a. REPORT SECURITY CLASSIFICATION UNCLASSIFIED		1b. RESTRICTIVE MARKINGS NONE	
2a. SECURITY CLASSIFICATION AUTHORITY		3. DISTRIBUTION / AVAILABILITY OF REPORT Approved for Public Release; Distribution Unlimited	
2b. DECLASSIFICATION / DOWNGRADING SCHEDULE		5. MONITORING ORGANIZATION REPORT NUMBER(S) NPS72-86-004CR	
4. PERFORMING ORGANIZATION REPORT NUMBER(S) NPS72-86-004CR		5. MONITORING ORGANIZATION REPORT NUMBER(S) NPS72-86-004CR	
5a. NAME OF PERFORMING ORGANIZATION JOSEPH FALCOVITZ	6b. OFFICE SYMBOL (If applicable) 72	7a. NAME OF MONITORING ORGANIZATION NAVAL POSTGRADUATE SCHOOL, CODE 72	
6c. ADDRESS (City, State, and ZIP Code) Research Contractor Naval Postgraduate School, Code 72 Monterey, CA 93943-5100		7b. ADDRESS (City, State, and ZIP Code) Space Systems Academic Group Monterey, CA 93943-5100	
8a. NAME OF FUNDING / SPONSORING ORGANIZATION Strategic Defense Initiative Office	8b. OFFICE SYMBOL (If applicable) SDIO/DEO	9. PROCUREMENT INSTRUMENT IDENTIFICATION NUMBER MIPR DGAA60045	
8c. ADDRESS (City, State, and ZIP Code) SDIO/DEO Washington, DC 20301-7100		10. SOURCE OF FUNDING NUMBERS	
		PROGRAM ELEMENT NO. PE63221	PROJECT NO.
		TASK NO.	WORK UNIT ACCESSION NO.
11. TITLE (Include Security Classification) Impulsive Loading From A Bare Explosive Charge in Space			
12. PERSONAL AUTHOR(S) JOSEPH FALCOVITZ			
13a. TYPE OF REPORT Contractor Report	13b. TIME COVERED FROM Jan 86 TO June 86	14. DATE OF REPORT (Year, Month, Day) December 1986	15. PAGE COUNT 65
16. SUPPLEMENTARY NOTATION			
17. COSATI CODES		18. SUBJECT TERMS (Continue on reverse if necessary and identify by block number)	
FIELD	GROUP	SUB-GROUP	
		Space Blast, Impulsive Loading, Explosive in Space	
19. ABSTRACT (Continue on reverse if necessary and identify by block number)			
<p>Consider a planform target subjected to a normal impact of explosive products generated by detonating a bare charge in space. It is suggested that the loading impulse may be approximated by the total momentum of that portion of the fluid which impacts at the target. Assuming impulsive dynamic response, and assuming that the ensuing damage is proportional to the kinetic energy imparted to the structure by the blast, we get a particularly simple law: $\text{Damage} \sim W^2/R^4$ (W is charge mass, R is range). This model is an idealization of a solar panel (or antenna) extended in a paddle-like fashion from a relatively rigid and massive core structure. It is also shown that this law implies that no advantage can be realized by re-arranging the mass of a single bare charge in a cluster configuration of smaller sub-charges, which would be dispersed and detonated via an idealized "isotropic" scheme.</p>			
20. DISTRIBUTION / AVAILABILITY OF ABSTRACT <input checked="" type="checkbox"/> UNCLASSIFIED/UNLIMITED <input type="checkbox"/> SAME AS RPT <input type="checkbox"/> DTIC USERS		21. ABSTRACT SECURITY CLASSIFICATION UNCLASSIFIED	
22a. NAME OF RESPONSIBLE INDIVIDUAL ALLEN E. FUHS, Distinguished Professor		22b. TELEPHONE (Include Area Code) (408)646-2948	22c. OFFICE SYMBOL

ABSTRACT

Consider a planform target subjected to a normal impact of explosive products generated by detonating a bare charge in space. It is suggested that the loading impulse may be approximated by the total momentum of that portion of the fluid which impacts at the target. Assuming impulsive dynamic response, and assuming that the ensuing damage is proportional to the kinetic energy imparted to the structure by the blast, we get a particularly simple law: $\text{Damage} \sim W^2/R^4$ (W is charge mass, R is range). This model is an idealization of a solar panel (or antenna) extended in a paddle-like fashion from a relatively rigid and massive core structure. It is also shown that this law implies that no advantage can be realized by re-arranging the mass of a single bare charge in a cluster configuration of smaller sub-charges, which would be dispersed and detonated via an idealized "isotropic" scheme.

ACKNOWLEDGEMENTS

DUDLEY KNOX LIBRARY
NAVAL POSTGRADUATE SCHOOL
MONTREALE, CALIFORNIA 93943-5002

This work is part of a study involving gas dynamics of exhaust plumes from spacecrafts. It was conducted under the cognizance of Distinguished Professor Allen E. Fuhs, who suggested extending our understanding of gasdynamics in space to the treatment of blast effects on spacecrafts. I wish to thank Professor Fuhs for his creative guidance and deeply appreciate his continuous support. The GRP code used for the blast computation is a product of mutual research conducted by Professor M. Ben-Artzi and myself. The fruitful collaboration of Professor Ben-Artzi is gratefully acknowledged.

TABLE OF CONTENTS

1.	INTRODUCTION.....	1
2.	IMPACT BLAST LOADING	3
3.	TARGET DYNAMIC RESPONSE.....	10
4.	CLUSTER CONFIGURATION.....	13
5.	DISCUSSION AND CONCLUSIONS	15
6.	REFERENCES	16
	APPENDIX A. The GRP Code.....	17
	A.1 Array Variables.....	18
	A.2 Major Parameters.....	20
	A.3 Labeled COMMON variables.....	21
	A.4 Description of Subroutines	24
	A.5 Listing of GRP Code.....	29
	APPENDIX B. Code for Re-Normalizing the Air Impulse.....	56
7.	DISTRIBUTION LIST	57

LIST OF FIGURES

Figure 2-1	Impact Blast Loading	7
Figure 2-2	Shock Reflection at Impact Phase.....	8
Figure 2-3	Limiting Cases of Shock Reflection (a) Initially Reflected Shock (Impact) (b) Stationary Shock	8
Figure 2-4	Impulse of Normally Reflected Blast Wave at Sea-Level and in Space	9
Figure 3-1	Cantilever Beam with Plastic Hinge.....	12
Figure 3-2	ChargeMass - Range - Damage Curves for Cantilever Beam.....	12
Figure 4-1	Target Intercept at Closest Approach.....	14
Figure 4-2	Spherical Cap Surrounding the Target.....	14
Figure A-1	Piecewise Linear Distribution of Flow Variables in Cells.....	53
Figure A-2	Intersection of Right and Left Adiabats for Solving Riemann Problem	54
Figure A-3	Wave Diagram Representing Solution to Riemann Problem.....	55

NOMENCLATURE (consistent units in m, kg, ms system)

C	Coefficient in Charge-Mass-Range-Damage relationship ($\text{m kg}^{-1/2}$)
D_{CJ}	Speed of propagation of detonation wave at CJ point (m ms^{-1})
I	Impulse per unit area of target ($\text{kg m}^{-1} \text{ms}^{-1}$)
\hat{I}	Dimensionless impulse $\hat{I} = I(R) [4\pi R_0^2 / W(2Q_0)^{1/2}]$
h	Beam thickness (m)
L	Length of cantilever beam (m)
m	Lagrange mass coordinate (kg)
M_p	Moment per unit length of plastic hinge (MPa m^2)
N	Number of sub-charges in a cluster configuration
P	Pressure (MPa)
P_s	Surface pressure (MPa)
Q_0	Explosive energy per unit mass (MJ kg^{-1})
R_0	Radius of spherical charge (m)
R	Range from center of charge (m)
S	Speed of propagation of shock wave (m ms^{-1})
t	Time (ms)
U	Flow velocity (m ms^{-1})
V	Velocity imparted to target by loading impulse (m ms^{-1})
W	Charge mass (kg)
Y	Plastic yield stress (MPa)
Z	Total momentum of an explosive charge (kg m ms^{-1})
α	Coefficient for dynamic pressure recovery
γ	Specific-heat ratio
γ_{CJ}	Specific-heat ratio of explosive products at CJ point
θ	Plastic rotation angle of cantilever beam
κ	Impact approximation impulse coefficient (presently $\kappa = 1$)
μ	Beam mass per unit area (kg m^{-2})
ρ	Fluid density (kg m^{-3})
ρ_p	Beam density (kg m^{-3})
φ	Mid-area angle of sub-charge spherical cap

EMPTY PAGE

1. INTRODUCTION

The advent of space-based weapon systems in our times has raised the prospects of future "Star Wars" conflicts, rendering the potential use of explosive devices against space targets a present day engineering reality. The warhead of choice in space seems to be of the fragmentation type, for obvious reasons. The effectiveness of fragments is unhampered by the space environment (lack of air may even be helpful). By contrast, bare charges in space are considerably less efficient than in air. One may wonder why this is so since in air, as in space, the same amount of chemical energy is released through the detonation process. The explanation is that the difference is in the much larger mass involved in the air blast, relative to the bare charge mass.

For a more comprehensive explanation, we take a close look at the process by which an explosive-driven air blast wave is generated. The explosive products effectively constitute a rapidly expanding spherical piston (typical initial speed around 6 km/sec), which drives an intense shock wave into the surrounding air. At a typical range of $100R_0$ (and with air density equal to about 1/1000 of charge density), the mass of air entrained by the shock is about 1000 times the charge mass. Thus, the highly concentrated initial explosive energy, has spread over a much larger mass than that of the charge, via the mechanism of wave propagation in compressible media, resulting in an increased momentum. For a comprehensive treatment of blast waves in air the reader is referred to Baker[1].

It is also worthwhile noting that explosive products in space typically attain hypersonic speed prior to impacting at the target. The flow velocity in an air blast is typically subsonic or somewhat supersonic. It is thus expected that the actual gasdynamic interaction between the blast flow and a stationary target, will be fundamentally different in these two cases.

We contend that blast effects in space may still be of practical interest for reasons such as the following :

- (i) Notwithstanding the poor efficiency of a bare charge, its use should not be ruled out altogether. Fragments would contribute to existing - and potentially hazardous - population of space debris, underlining the obvious fact that there is no absolutely safe standoff distance from an isotropic fragmentation warhead. A clean bare charge may thus be a reasonable alternative.
- (ii) Even a fragmentation warhead has some residual blast capacity, which has to be considered either as a factor in enhancing target damage, or as a threat to be reckoned with in determining a safe standoff distance.

The key idea of the present model is a combination of the assumption that target dynamic response is related primarily to total blast impulse, and the physically plausible notion that this impulse is equal to the total momentum of that portion of the expanding explosive products which impacts at the target. The sense in which this simple notion constitutes an approximation to a proper gasdynamic analysis of the interaction between the fluid and the target, is clarified in Ch. 2. In that chapter we also present an illuminating comparison between impulsive blast loading in air and in space.

In order to demonstrate the Charge-Mass-Range-Damage relationship implied by our impact blast approximation, we chose a simple target model: A cantilever beam with a rigid-perfectly plastic stress-strain relationship. It represents an extended structural element such as a solar panel or an antenna. We make use of studies conducted by Mentel [2] and by Bodner and Symonds [3], which showed that by and large, the effect of accelerating the beam impulsively was to cause a rotation about a plastic hinge at the point of support. The final angle of rotation is generally proportional to the initial kinetic energy, so that equating damage with that angle, results in damage being proportional to the square of the impulse imparted to the target by the blast loading. A presentation of this dynamic response model, including a sample case, is given in Ch. 3.

Our Charge-Mass-Range-Damage relationship may imply some far-reaching conclusions when applied to the analysis of a more general configuration than the single-charge/single-target case. In Ch. 4 we present a simple analysis of a sub-munition configuration of N bare charges, concluding that it seems to have no advantage in efficiency, relative to a single charge of equal mass. Sections 5 and 6 contain conclusions and references, correspondingly.

We conclude the introduction by listing the main assumptions made in the present study:

- (a) Blast loading and target response are uncoupled. This is true since typically the target mass is much larger than the mass of that portion of the explosive products which impacts on it.
- (b) Dynamic target response is independent of specific loading time history. It depends solely on total (time-integrated) impulse.
- (c) The target is a panel extended as a relatively supple cantilever. It is supported by a relatively rigid and massive core structure.
- (d) The charge is a sphere detonated at its center. The expansion is spherically symmetric.
- (e) Target surface is normal to local flow vector.
- (f) Target orbital velocity relative to the center of the charge is negligible, compared with the velocity of the expanding products.

2. IMPACT BLAST LOADING

Consider the expanding explosive products impacting at a target as shown in Fig. 2-1. By regarding the fluid as an ensemble of non-interacting particles moving at velocity $U(R,t)$, and by assuming a no-rebound normal impact at the surface, the pressure time history is given by :

$$P_s(t) = \rho(R,t)[U(R,t)]^2 \quad (2-1)$$

How is this simple impact mechanism related to the actual gasdynamic interaction between the expanding explosive products and the target? When a target is located at a range of at least several charge radii, two features in the free stream of the oncoming fluid are significant : The flow is highly hypersonic (Mach number 20 or higher), and the static pressure is very small, which means that $P + \rho U^2 \approx \rho U^2$. These facts were born out by a numerical computation which we performed for a typical high explosive characterized by the following parameters :

$$\rho_0 = 1800 \text{ (kg m}^{-3}\text{)}$$

$$\gamma_{CJ} = 3$$

$$D_{CJ} = 8 \text{ (m ms}^{-1}\text{)}$$

$$Q_0 = D_{CJ}^2 / [2(\gamma_{CJ}^2 - 1)] = 4 \text{ (MJ kg}^{-1}\text{)}$$

(2-2)

Where Q_0 was determined by assuming that the detonation corresponded to the CJ point on the explosive Hugoniot curve, and that the detonation products were an ideal gas with a specific-heat ratio γ_{CJ} . The spherically expanding flow was computed by integrating the Euler equations for isentropic flow via a high-resolution conservative finite-difference scheme [4-6]. The initial conditions were the self-similar flow field of a just-detonated spherical charge given by Taylor [7]. The code GRP with which the computation was performed is described and listed in Appendix A.

Consider the flow at a stationary target, which begins at the moment of arrival of the expanding explosive products (Fig. 2-2). A qualitative description of the ensuing flow pattern is made by observing its evolution in time. Immediately following the initial (normal) impact, the fluid is stopped at the target by a backward-propagating shock wave reflected from the surface. Since the target is of

finite extent, the fluid between the shock and the surface is accelerated laterally, and streamlines that tend to curve around the target are being formed. If the oncoming flow were stationary, the flow field would evolve toward the familiar configuration of a detached bow-shock positioned at a relatively narrow standoff distance from the surface.

Let us find the post-shock pressure in these two limiting phases. In the initial phase, the fluid is stopped at the target by a reflected shock (Fig. 2-3a), and in the pseudo-stationary phase (Fig. 2-3b), the shock is stationary. In either case we find the post-shock pressure to be given by a pressure-recovery expression of the form :

$$P_2 = \alpha \rho U^2 \quad (2-3)$$

Where α is a constant related to the appropriate γ (assuming the expanded explosive products are an ideal gas). The governing equations in the reflected shock case are :

$$\rho(U+S) = \rho_2 S$$

$$\rho(U+S)^2 = P_2 \quad (2-4)$$

$$\rho(\gamma + 1)/(\gamma - 1) = \rho_2 \quad (\text{strong shock})$$

Where the unknowns are ρ_2 , P_2 , S .

The equations for the stationary shock case are :

$$\rho U = \rho_2 U_2$$

$$\rho U^2 = P_2 + \rho_2 U_2^2 \quad (2-5)$$

$$\rho(\gamma + 1)/(\gamma - 1) = \rho_2 \quad (\text{strong shock})$$

Where the unknowns are ρ_2 , U_2 , P_2 . Thus, solving for α in the two cases represented by equations (2-4) and (2-5), we get :

$$\begin{aligned} \text{Reflected shock} \quad \alpha &= [(\gamma + 1)/2]^2 \\ \text{Stationary shock} \quad \alpha &= 2/(\gamma + 1) \end{aligned} \tag{2-6}$$

In either case, since the gas is not dense, the effective range of γ is somewhere between 1.0 and 1.4, so that setting $\alpha = 1$ is an approximation commensurate with the overall crudeness of the present impact blast model. Since the flow in the layer between the shock and the target is low subsonic (at least it is so away from target edges), the post-shock pressure is a reasonable substitute for the surface pressure. Also, $\alpha = 1$ is an appropriate approximation where the flow is so rarefied that it is collisionless. In this limit, $\alpha = 1$ corresponds to full thermal accommodation of re-emitted molecules from a presumably cold surface.

The foregoing analysis constitutes a justification of the impact approximation to the surface pressure (2-1). Now we turn to the task of evaluating the impulse which is defined as the time-integrated surface pressure. Using the impact approximation (2-1), the impulse is given by :

$$I(R) = \int_0^{\infty} P_s(t) dt = \int_0^{\infty} \rho(R,t) [U(R,t)]^2 dt \tag{2-7}$$

Let us introduce a Lagrange mass coordinate m which enables a transformation from the Euler system (R,t) to the Lagrange system (m,t) . The differential relation associated with this transformation at constant R is :

$$dm = 4\pi R^2 \rho(R,t) U(R,t) dt \tag{2-8}$$

Since it is assumed that the fluid is not accelerated at any (R,t) in the range of interest for blast loading, the velocity $U(R,t)$ can be regarded as function *solely of the mass coordinate*, so that $U(R,t) = U(m)$. Using (2-8) we are then able to cast the impact blast expression (2-7) in the following simple and physically appealing form :

$$\begin{aligned} I(R) &= Z/4\pi R^2 \\ Z &= \int_0^W U(m) dm \end{aligned} \tag{2-9}$$

The upper limit W in (2-9), which is consistent with the upper limit ∞ in (2-7), implies that the total impulse is somewhat overestimated, since it contains contributions from the innermost layers of the explosive products that will arrive at the target as $t \rightarrow \infty$.

The total momentum Z is thus a constant which can be evaluated for any specific explosive charge by numerical integration. We performed this computation with the code GRP described in Appendix A. In doing so for the typical explosive (2-2), we found out that the impulse (2-9) was a reasonable approximation at ranges as low as $R = 3R_0$. Furthermore, it was found that Z could be approximated by the maximum attainable momentum for the given charge mass and energy $W(2Q_0)^{1/2}$, to within about 6%. Apparently, the total momentum is not overly sensitive to the exact velocity distribution function $U(m)$, so that assuming a value of Z appropriate to the uniform distribution $U(m) = (2Q_0)^{1/2}$ is a reasonable approximation. Thus we finally arrive at the following closed-form approximation for the blast impulse :

$$I(R) = \kappa W(2Q_0)^{1/2}/4\pi R^2 \quad (2-10)$$

$$\kappa = 1$$

Where the coefficient κ is retained in order to suggest that its value be determined more accurately from detailed experimental or computational data, in the event that such data become available. At present our best estimate is $\kappa = 1$.

There is one comparison, however, which can readily be made with available data. We refer to impulsive blast loading in air, such as given by Baker (Ref. 1, Fig. 6.3 in the supplement). The comparison is conveniently made with a non-dimensional form of (2-10), which is rewritten as :

$$\hat{I} = I(R) [4\pi R_0^2/W(2Q_0)^{1/2}] = (R/R_0)^2 \quad (2-11)$$

The air blast data has to be converted to the same normalization scheme as in Eq. (2-11), before the comparison can be made. Considering the definition of \hat{I} in (2-11) above, and the definition of scaled range and air blast impulse (Table 6.2 of Ref. 1), this conversion is done by multiplying the scaled air impulse and range by the following coefficients (sea-level air is assumed) :

Impulse Multiplier	$\beta = 3(2\gamma)^{-1/2}(4\pi/3)^{1/3} (P_a/\rho_a Q_0)^{1/6} (\rho_a/\rho_0)^{1/2} = .01204$	
Range Multiplier	$\delta = (4\pi/3)^{1/3} (\rho_0 Q_0/P_a)^{1/3} = 67.06$	(2-12)
$\rho_a = 1.3 \text{ (kg m}^{-3}\text{)}$	$P_a = 0.1 \text{ (MPa)}$	$\gamma = 1.4$

The air blast conversion was done by a small code which is given in Appendix B. The air and space blast impulses are shown in Fig. 2-4. We note that at ranges larger than about 10 charge radii, the air blast impulse is higher than the space impulse, and the gap widens as the range increases. This observation is consistent with the qualitative explanation given in the introduction, which attributed this effect to the increase in the entrained air mass at higher range. At ranges lower than 10 charge radii, the air mass is relatively insignificant, so that one may expect the blast impulses in air and in space to be comparable. Indeed, the inverse-square variation of impulse with range is apparent for the air blast at low range. In absolute values, however, the low-range space impulse is higher by a factor of about 1.7. This might be interpreted as indicating that choosing $\kappa = 1/1.7$ would be the appropriate "calibration". However, we do not propose to do so, since we are not able to trace the various factors affecting the low-range impulse as given by Baker [1]; they may somehow depend on the presence of air, as well as on other parameters such as target size and equation of state of the explosion products.

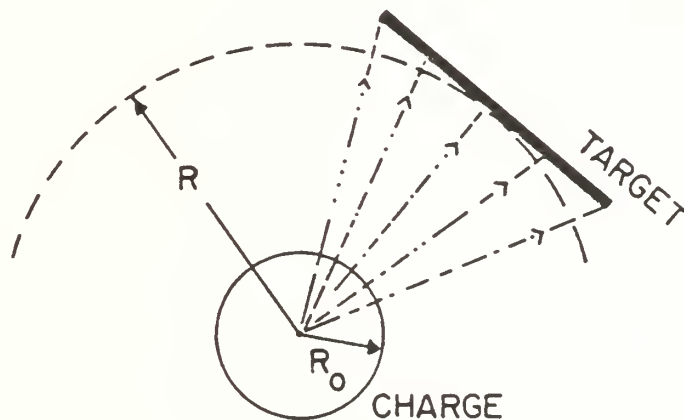


Figure 2-1. Impact Blast Loading

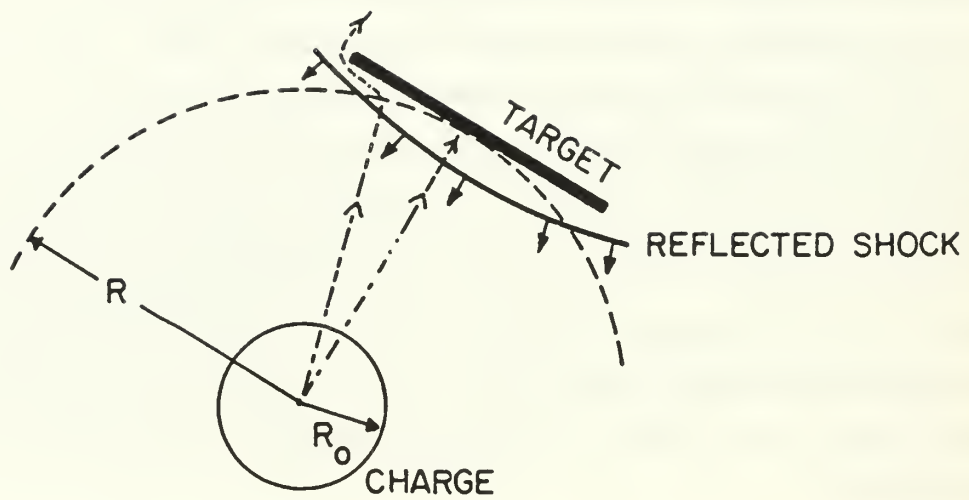


Figure 2-2. Shock Reflection at Impact Phase

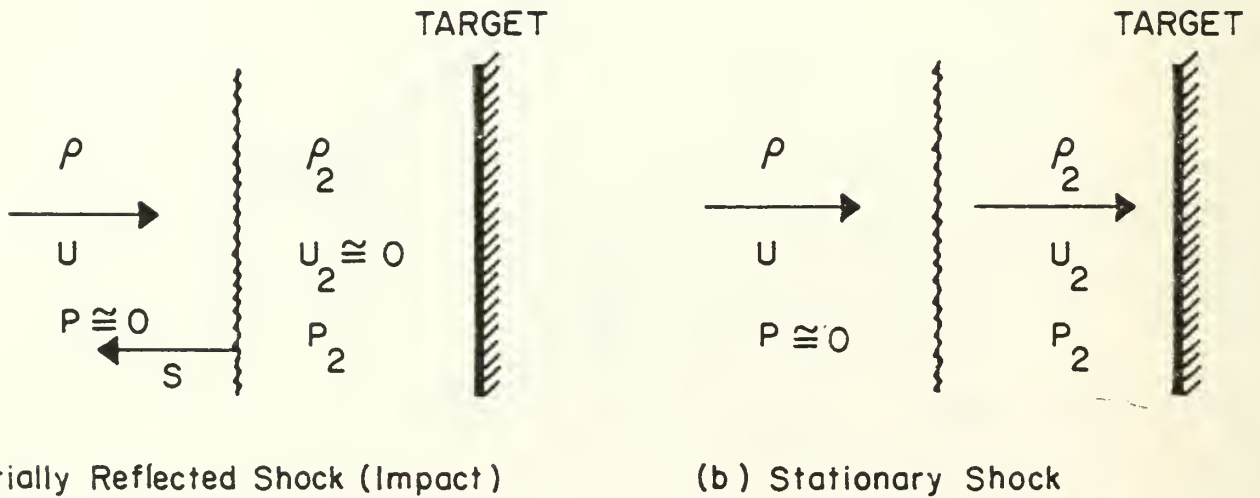


Figure 2-3. Limiting Cases of Shock Reflection

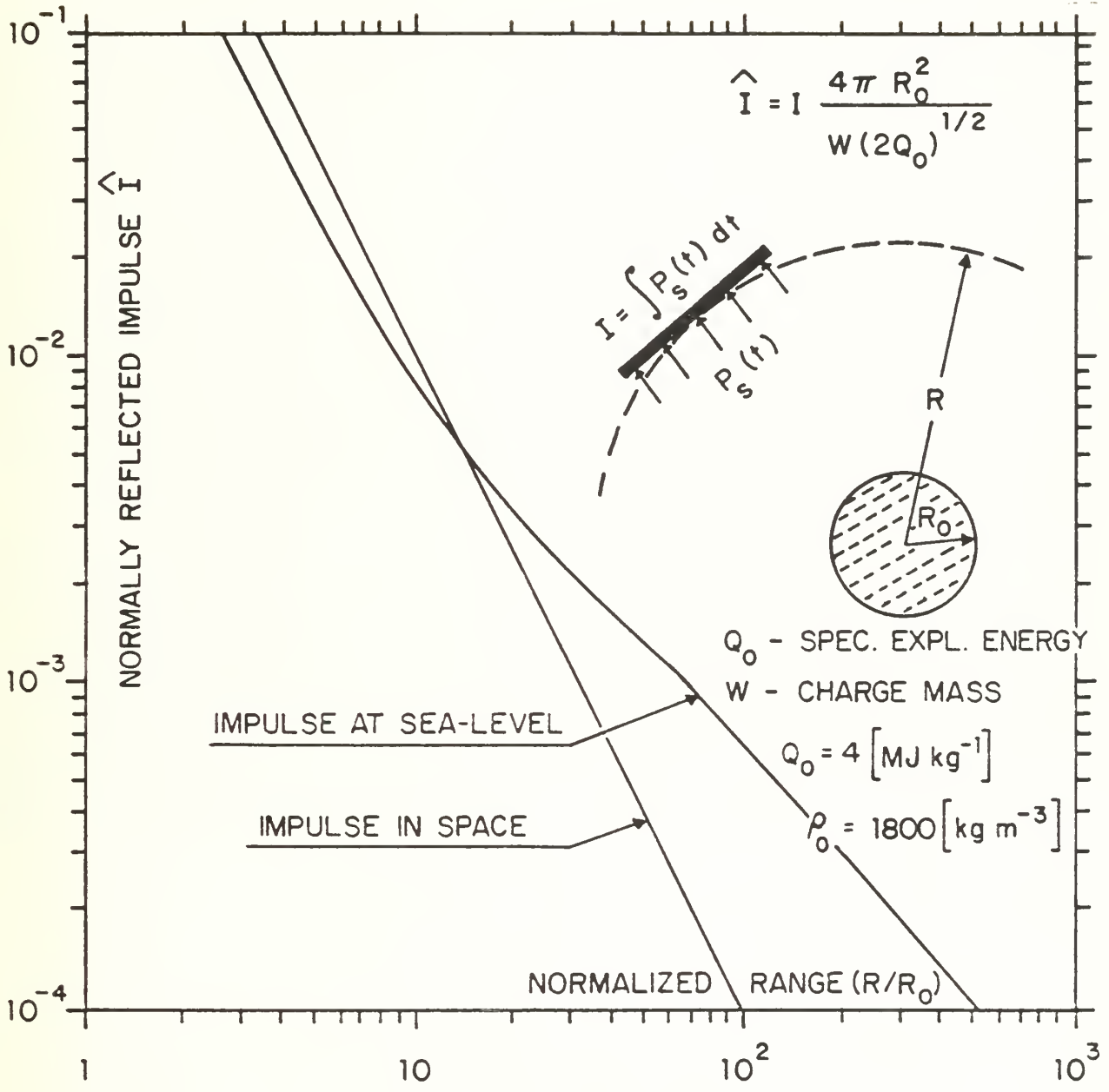


Figure 2-4. Impulse of Normally Reflected Blast Wave at Sea-Level and in Space

3. TARGET DYNAMIC RESPONSE

For the sake of constructing representative Charge-Mass-Range-Damage relations from our impact approximation to the blast impulse (2-10), we suggest a simple idealized structure as target model. It is a cantilever beam made of a metal characterized by a rigid-perfectly plastic stress-strain relation.

This model is supposed to represent an extended spacecraft component such as a solar panel or an antenna. The core structure is assumed to be much more massive and rigid than the extended structural element, so that the cantilever can be idealized as being rigidly supported. The sole dynamic and structural parameters are hence those of the cantilever.

For this purpose we make use of an experimental and theoretical investigation of uniform cantilever beams subjected to impulsive loading that was conducted by Mentel [2]. Aluminum alloy beams were held in a massive support that was gliding along a rail at speed V , until it was abruptly stopped by a very massive anvil. After the system came to rest, the beams were observed to have rotated through an angle θ about the point of support, with little deformation elsewhere (Fig. 3-1).

The theoretical model suggested by Mentel [2] for predicting $\theta(V)$, can be described as comprising two stages. Immediately following the impact, the beam commences rotating rigidly about the support point, with an angular momentum equal to the pre-collision moment of momentum about that point. This application of the principle of conservation of moment of momentum entails an abrupt re-distribution of velocity in the beam, with velocity being proportional to distance from support, and the tip moving at $1.5 V$. The angle θ is subsequently determined from the requirement that the rotational kinetic energy be dissipated as plastic hinge work $M_p \theta$. The resulting $\theta(V)$ expression is :

$$\theta = (3/8)\mu LV^2/M_p \quad (3-1)$$

We now make one more step in formulating the model, in that we postulate that *the angle θ is a measure of damage*. Using the following expressions for M_p , μ and V :

$$M_p = (1/4)Yh^2$$

$$\mu = \rho_p h \quad (3-2)$$

$$V = I(R)/\mu$$

We get from (2-10) and (3-1) the following Charge-Mass-Range-Damage ($W-R-\theta$) relationship :

$$R = CW^{1/2} \tag{3-3}$$

$$C = [(3/16\pi^2\theta) (LQ_0/\rho_p Yh^3)]^{1/4}$$

We note that the effective range for a specified target and "damage level" θ , is proportional to the square root of the charge mass W .

Using the data for the typical explosive (2-2), and the following data for a specific aluminum beam, we get for this sample case :

$$h = 0.002 \text{ (m)}$$

$$L = 1.0 \text{ (m)}$$

$$\rho_p = 2700 \text{ (kg m}^{-3}\text{)} \tag{3-4}$$

$$Y = 300 \text{ (MPa)}$$

$$C = 1.85 \theta^{-1/4} \text{ (m kg}^{-1/2}\text{)}$$

The Charge-Mass-Range-Damage relationship corresponding to this sample case is depicted in Fig. 3-2.

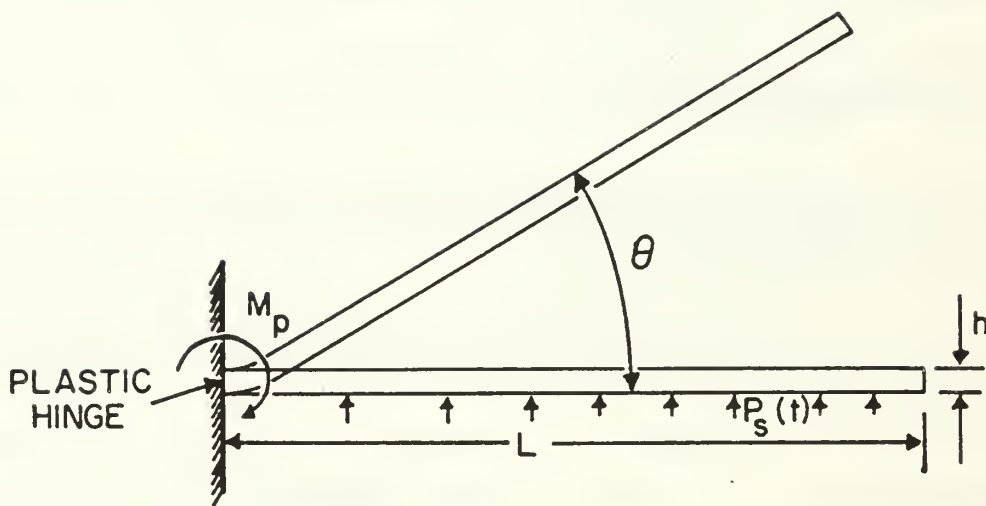


Figure 3-1. Cantilever Beam with Plastic Hinge

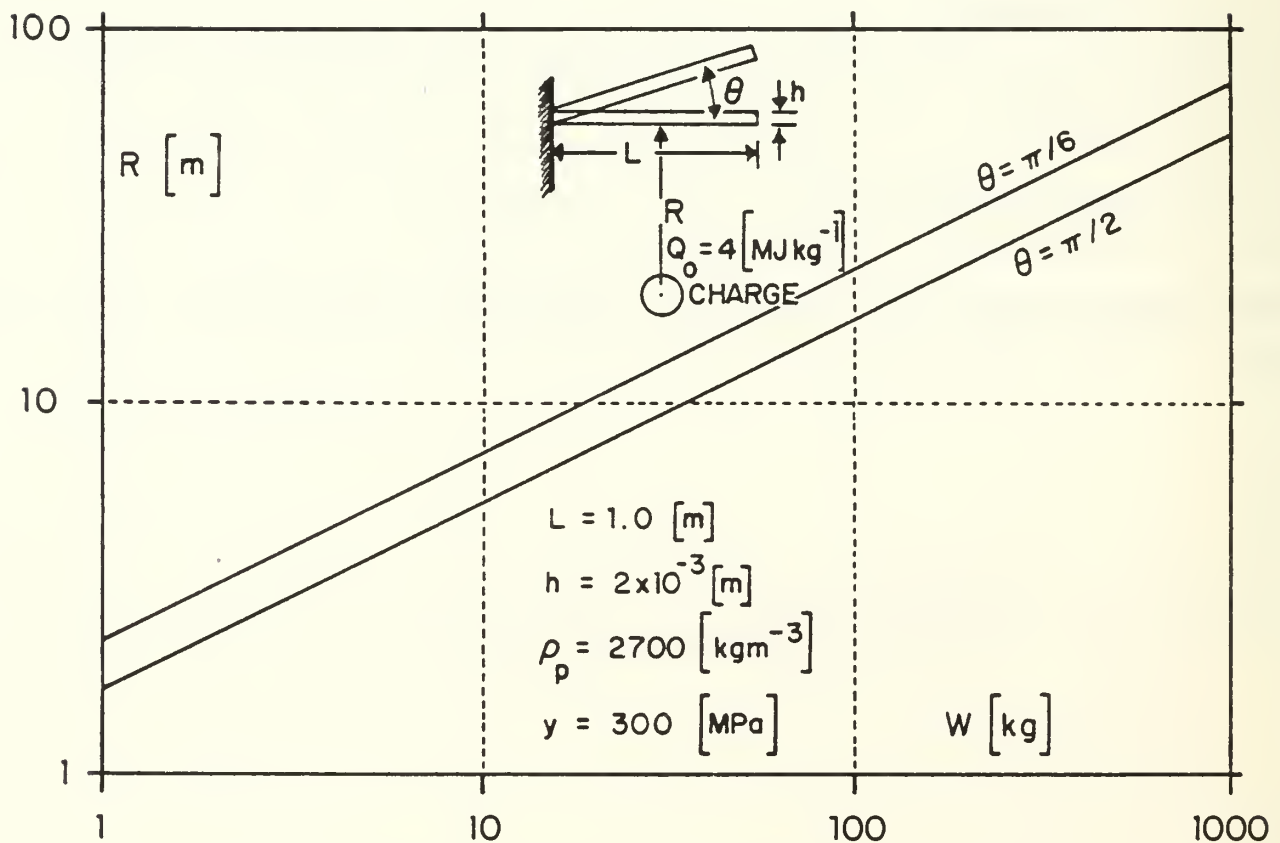


Figure 3-2. Charge Mass - Range - Damage Curves for Cantilever Beam

4. CLUSTER CONFIGURATION

In a cluster configuration, the gain in damage is presumably a result of a favorable design tradeoff between reduced charge mass and reduced range. Can such a gain be achieved for a space system, assuming the ChargeMass-Range-Damage law (3-3) to hold? It can be shown that by adopting some simple strategy of sub-munition dispersion and initiation, equation (3-3) implies no gain in target damage.

Let us assume for the sake of a reasonably simple analysis, that dispersion and initiation of sub-charges would take place according to the following scheme :

- (a) The N sub-charges appear to fan out from a common virtual center, moving at equal speeds. At subsequent times, their centers are uniformly distributed over an expanding spherical envelop.
- (b) The target moves at a constant velocity relative to the virtual center. Its point of closest approach to that center is at range R .
- (c) The timing for dispersion is chosen so that the target intersects (tangentially) with the spherical envelop at the point of closest approach (Fig. 4-1). This is also the point at which the blast from a single-charge configuration detonated at the virtual center, would have impacted at the target.
- (d) All sub-munitions are detonated at this "moment of closest approach".
- (e) It is assumed that each spherical cap of area $4\pi R^2/N$ will contain one, and only one, sub-charge. The probability of the charge location on that cap is assumed to be uniformly distributed. The expected location on the cap is hence that latitude line φ which divides the cap into two parts of equal area (Fig. 4-2).
- (f) It is assumed that the target is subjected to the blast of a single sub-charge, which is located on the mid-area latitude φ of the spherical cap that surrounds the target (Fig. 4-2).

Since the area of the spherical cap subtended by φ is $4\pi R^2/(2N)$, the angle φ is given by :

$$\sin(\varphi/2) = (2N)^{-1/2} \quad (4-1)$$

We seek a comparison between the deflection θ for a single charge (W,R) , and the deflection θ_N in the sub-munition case ($W_N = W/N$, $R_N = 2R\sin(\varphi/2)$). From the ChargeMass-Range-Damage law (3-3), using also Eq. (4-1), we get :

$$(\theta_N/\theta) = (W_N/W)^2 (R/R_N)^4 = 1/4 \quad (4-2)$$

Consequently, there is no potential gain in a tradeoff between charge mass and range, for a cluster configuration with the aforementioned dispersion scheme. The factor 1/4, along with the mass overhead inherent in constructing a multi-charge configuration, indicate that in causing blast damage, a single charge is more effective than an equal-mass isotropically dispersed cluster.

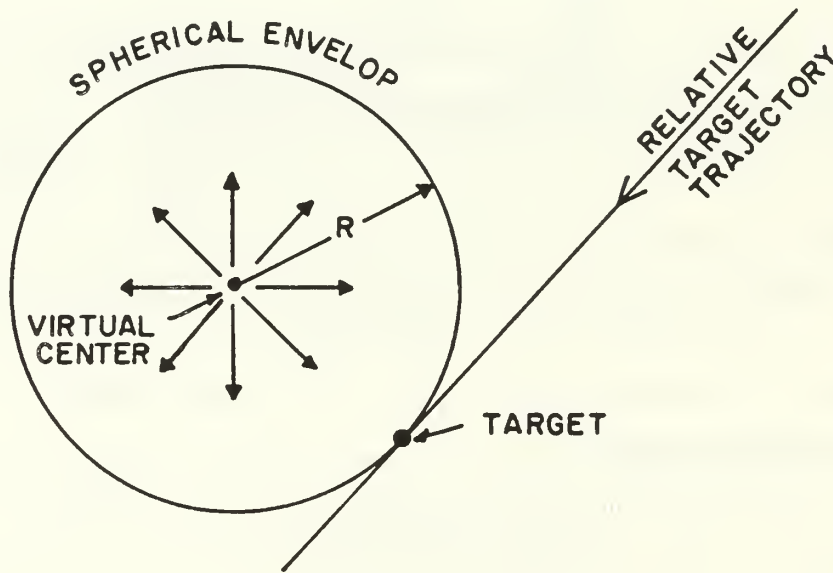


Figure 4-1. Target Intercept at Closest Approach

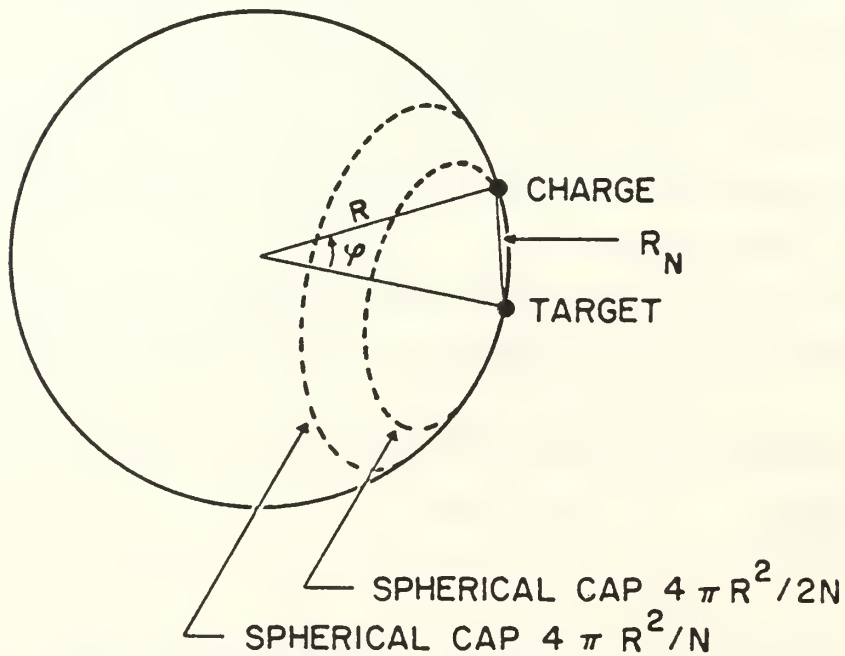


Figure 4-2. Spherical Cap Surrounding the Target

5. DISCUSSION AND CONCLUSIONS

Our analysis pertains to a bare explosive charge initiated at a point of closest approach to the target. We have shown that the loading impulse on a planform target is given by the impact approximation (2-7), which states that the impulse is proportional to the charge mass and inversely proportional to the range squared. The impulse in space has been compared with impulse in air at sea-level. It was found that the two are quite comparable at close range (10 charge radii or less), exhibiting identical variation with range. At far ranges, the impulse in air is the higher one. This is consistent with the notion that spreading the explosive energy over larger air mass results in larger momentum (and hence reflected impulse). We then proceeded to develop the ChargeMass-Range-Damage law (3-3) for an impulse-responsive target, which states that blast damage is proportional to the square of the charge mass and inversely proportional to the fourth power of the range. These results were obtained by introducing extensive simplifications in the analysis of gasdynamic interaction, and in the analysis of dynamic target response. We have further shown that this damage law also implies that no gain can be achieved by an idealized cluster configuration of bare sub-charges, relative to a single charge of equal total mass.

It is worthwhile noting that all assumptions introduced in the course of formulating the impact blast approximation and the structural dynamic response to impulsive loading, imply that target damage is overestimated. The only exception is the approximation in setting $\alpha = 1$, which can be readily rectified by assigning to α the reflected shock value given in (2-6). Furthermore, we assumed that the pressure at the midpoint of the target, is the pressure everywhere on the target. Due to flow around the edges, the average pressure is lower than the midpoint pressure. Also, targets are not everywhere normal to the flow (and charge/target attitude is not a design parameter). Oblique impact obviously entails reduced target loading. In the area of structural dynamic response, a time-distributed loading function generally delivers less kinetic energy to the structure than an impulsive loading of equal total impulse, resulting in reduced deformation (damage). Thus, while the present model may be regarded as an over estimate when applied to a sure-fail analysis, it is particularly suitable in determining a sure-safe range.

6. REFERENCES

- [1] Baker, W. E., Explosions in Air , University of Texas Press, Austin and London, 1973.
- [2] Mentel, T. J., "The Plastic Deformation Due to Impact of a Cantilever Beam with an Attached Tip Mass", Journal of Applied Mechanics, pp. 515-524, 1958.
- [3] Bodner, S. R. and Symonds, P. S., "Experimental and Theoretical Investigation of the Plastic Deformation of Cantilever Beams Subjected to Impulsive Loading", Journal of Applied Mechanics, pp. 719-728, 1962.
- [4] Ben-Artzi, M., and Falcovitz, J., "A High-Resolution Upwind Scheme for Qausi 1-D Flows", INRIA Workshop on *Numerical Methods for Solving the Euler Equations of Fluid Dynamics*, F. Angrand and R. Glowinski (editors), Paris, Dec. 1983, SIAM Publication, Philadelphia, 1985.
- [5] Ben-Artzi, M., and Falcovitz, J., "A Second-Order Godunov-Type Scheme for Compressible Fluid Dynamics", Journal of Computational Physics, Vol 55, pp.1-32, 1984.
- [6] Ben-Artzi, M. and Falcovitz, J., "An Upwind Second-Order Scheme for Compressible Duct Flows", SIAM Journal on Scientific and Statistical Computing, Vol 7, p.744-768, 1986.
- [7] Taylor, G. I., "The Dynamics of the Combustion Products Behind Plane and Spherical Detonation Fronts in Explosives", Proc. Roy. Soc. A, Vol CC (1950), pp.235-247. Also : The Scientific Papers of Sir Geoffrey Ingram Taylor, Vol III, G. K. Batchelor, Editor, Cambridge Press, 1963.

APPENDIX A. The GRP Code

The purpose of this Appendix is to provide a concise description of the GRP code, and a listing of its CHARGE version. It is intended for users that have had prior experience in implementing schemes for solving the Euler equation of compressible flow. The theoretical background of GRP schemes constitutes the principles on which the code is founded. Some familiarity (at least) with this background, as given in References 4, 5 and 6 is indispensable to any implementation of GRP schemes. Reference 4 is recommended as an introduction. The planar GRP scheme is fully described in Reference 5, and the duct-flow GRP scheme on which the present CHARGE version is based is given in Reference 6. (In CHARGE version the flow is spherical and the "duct" area is set to $X(I)**2$, but the code can handle any area variation - see subroutines CROSS and RATIO below).

In GRP schemes, second-order accuracy is achieved by considering a piecewise linear interpolation of the flow in each cell (Fig. A-1), from which second-order accurate fluxes at each cell interface are evaluated through an analysis of a local Generalized Riemann Problem (GRP). Briefly stated, the GRP goes one step further than the Riemann Problem (RP), in that it seeks (analytically) the first time-derivative of the flow that evolves as the "diaphragm" is removed from the cell interface, at the origin of the centered (X,T) wave paths of the RP solution. The major computational subroutines are CYCEUL where the integration of conservation laws is performed, RIEMAN where the local Riemann Problems are solved by Newton-Raphson iterations, MAGA where the closed-form expressions derived from the GRP analysis [6] are used to compute flow time-derivatives along the contact surface, FLUXE where all the previously computed information is used to extrapolate the fluxes to mid-time-step ($T + DT/2$) which constitutes a second-order accurate flux.

The plan of this Appendix is as follows. Array variables, including those which carry conserved variables (mass, momentum and energy), are described in section A.1. This is followed by descriptions of general parameters (A.2), labeled COMMON variables (A.3) and all subroutines (A.4). We conclude by giving the CHARGE version listing (A.5), which should be consulted whenever a reading of this code description is attempted.

NOTE : The present CHARGE version was implemented in a GRP code version that had been converted to treat detonation waves as chemically reactive compressible flow. However, the detonation scheme is effectively neutralized by setting QDET=0 (in NETUNM). All variables pertaining to detonation, such as arrays Z(I), DZ(I), FIMZ(I), ZMDOT(I) and labeled COMMON variables containing Z in their names, should be ignored.

A.1 Array Variables

The code GRP is organized so that all major subroutines are called with standard list of array variables which represent the integration scheme (i.e. the conservation laws), local Riemann Problem solutions and second-order accurate fluxes. Virtually all array variables are initially defined in BEGIN (initial conditions), and are subsequently updated at each time step in CYCEUL. The following list explains the meaning of these variables. Some terms used in the list are defined below.

X(I)	grid point coordinate.
U(I)	velocity in cell I.
P(I)	pressure in cell I (computed from equation of state).
RO(I)	density in cell I. This variable is time-integrated according to the law of conservation of mass. (Computed in CYCEUL).
E(I)	total energy per unit volume (including kinetic energy) in cell I. This variable is time-integrated according to the law of conservation of (total) energy. (Computed in CYCEUL).
DU(I)	velocity difference in cell I.
DP(I)	pressure difference in cell I.
DRO(I)	density difference in cell I.
DG(I)	Lagrange sound velocity difference in cell I.
DXSI(I)	the Lagrange coordinate increment defined as $RO(I)*(X(I+1)-X(I))$, for cell I.
MIN(I)	inactive in present version.
US(I)	velocity at the contact surface obtained after the resolution of the local discontinuity at X(I) (Riemann Problem solution). It is denoted as U^* in References 4-6.
PS(I)	pressure at the contact surface obtained after the resolution of the local discontinuity at X(I) (Riemann Problem solution). It is denoted as P^* in References 4-6.
UIDOT(I)	time derivative of US(I) along the contact surface. (This derivative is the result of the GRP analysis. It is computed in MAGA. See Ref. 5 and 6).
PIDOT(I)	time derivative of PS(I) along the contact surface. (This derivative is the result of the GRP analysis. It is computed in MAGA. See Ref. 5 and 6).
FIMZ(I)	inactive in present version.
ZMDOT(I)	inactive in present version.

TENA(I)	momentum per unit volume $RO(I)*U(I)$ in cell I. This variable is time-integrated according to the law of conservation of momentum. (Computed in CYCEUL).
FIRO(I)	mass flux at point X(I) (second-order accurate).
FIM(I)	momentum flux at point X(I) (second-order accurate).
FIE(I)	energy flux at point X(I) (second-order accurate).
GIP(I)	the pressure term in the momentum flux. It corresponds to G(U) in References 4 and 6.
VOL(I)	volume of cell I.
Z(I)	inactive in present version.
DZ(I)	inactive in present version.

Glossary of terms used in the array variables list :

Cell I - the cell between grid points X(I) and X(I+1). All cell variables are averages per that interval.

Difference in cell I - the difference between values of variable at cell boundaries X(I+1) and X(I). Those values are obtained from "monotonized" piecewise linear distribution of each variable in each cell. (Fig. A-1).

Second-order accurate flux - the flux time-derivative at point X(I) is computed from the time-derivatives of pressure and velocity along contact surface PIDOT(I) and UIDOT(I) (in FLUXE). Then the the flux is extrapolated to the centered time point $(T+DT/2)$, using those derivatives. This centered value is the second-order flux for integrating the conservation laws between T and T+DT.

A.2 Major Parameters

A list of major parameters indicating their meaning and the routine in which they are defined, is given below. Those parameters defined in NETUNM are the run input. There is no reading of an input file in this version of GRP code (and the only output is the printed output).

L	number of grid points + 1 (main program)
LL	L - 1 (MAIN PROGRAM)
T	time (MAIN0)
DT	time step (MAIN0)
TMAX	maximum time (when T.GE.TMAX the run is terminated) (NETUNM)
TMUD	time for which next printing will take place (NETUNM)
DTMUD	printing time step (NETUNM)
NCYC	serial number of time step (integration cycles) (MAIN0)
COLELA	switch to evaluate cell differences by Colella's method when COLELA.NE.0 (NETUNM)
KEYMON	key for monotonization scheme (just one is presently provided when COLELA.EQ.0) (NETUNM)
NCYCPR	frequency of line printing at each cycle (time step) (NETUNM)
STAB	CFL stability coefficient. Must be smaller than 1. (NETUNM)
DTBA	next time step computed from stability criterion (CYCEUL)
DTKOD	former time step (MAIN0)
KDT	index of cell where DTBA was determined (CYCEUL)

A.3 Labeled COMMON variables

Labeled COMMONs are used primarily to transmit data to and from routines that perform the major computational steps of the GRP scheme, i.e, RIEMAN, MAGA and FLUXE; these routines are called from CYCEUL. When the value of any of those variables is needed for later use, whether for updating conservation variables (RO, TENA, E), or for printing, it is stored in the appropriate array. All labeled COMMON variables are grouped under labels that indicate their role, and their names are also mnemonic. Generally, suffix L means Left and suffix R means Right. It may indicate sides either with respect to a cell interface X(I), or with respect to the contact surface which separates the Right- and Left- propagating waves in a solution to the local Riemann Problem. We indicate by INPUT variables that are computed prior to calling the subroutine, and by OUTPUT variables whose value was computed within the subroutine and constitutes the result of calling that subroutine.

COMMON /STEP0/ Parameters related to the local Riemann Problem. This is the first step in the GRP scheme.

UL, PL, ROL, CL, GL, SL - velocity, pressure, density, sound speed, Lagrange sound speed and entropy, attributed to Left side of cell interface at point X(I). (INPUT)

USTAR, PSTAR - velocity and pressure at the contact surface obtained when the local discontinuity is resolved (i.e., the solution to the local Riemann Problem). The omission of L or R suffix indicates that P and U are continuous across the contact surface. (OUTPUT)

RSTARL, CSTARL, GSTARL - density, sound speed and Lagrange sound speed on the Left side of the contact surface. (OUTPUT)

WL - Lagrange velocity of propagation of the Left-moving shock, relative to the fluid. (OUTPUT)

UW(6) - velocity of propagation of each wave front (Fig. A-3), relative to the inertial system (X). (OUTPUT)

HELEML - logical variable. If HELEMLEQ..TRUE. the Left-propagating wave is a shock. Otherwise it is a (centered) rarefaction wave. (OUTPUT)

NFLUX - integer variable. It denotes the region in the Riemann solution wave structure, which contains the point X(I) for all time. Refer to Fig. A-3 for illustration. (OUTPUT)

LAMDAL, RATEL, TEMPL, TEMPSL, ZL, ZSTARL - inactive.

COMMON /STEP1/ Parameters related to the time-derivative evaluation of the GRP scheme, performed in MAGA. The time-derivatives of P and U along the contact surface are the main result of MAGA.

DUIDT, DPIDT - time-derivatives of velocity and pressure along contact surface. (OUTPUT)

ASTARL - The directional derivative of U along the fan characteristic at the trailing characteristic of the Left rarefaction wave. It is not evaluated when the Left wave is a shock. (See References 4-6) (OUTPUT)

DGIDTL, DRIDTL - time-derivatives of Lagrange sound speed and density along the left side of the contact surface. (OUTPUT)

DSDAL - Lagrange spatial derivative of entropy on the left side of contact surface, prior to removal of the partition at X(I).

SH, RAT - the cross-section area and the x-derivative of $\ln(\text{SH})$. They are user-defined in CROSS and RATIO respectively.

DSDASL - entropy derivative used in the special "sonic" case (i.e, when NFLUX=2 or NFLUX=5). See References 5,6 for details. (OUTPUT)

LAMDSL, DZDAL, BETACL, DZDASL - inactive.

COMMON /GRADS/ Used to transmit flow gradients (that exist in fluid prior to removal of the partition at X(I)) to MAGA.

DUDXIL, DPDXIL, DGDXIL, DRDXIL, DSDXIL - gradients of U, P, G, RO, S (with respect to Lagrange coordinate). They are computed in CYCEUL for transmission to MAGA. (INPUT)

DZDXIL - inactive.

COMMON /FI/ Used to return values of updated flux and cell-interface variables from FLUXE.

FIH1, FIH2, FIH3 - second-order flux of mass, momentum flow (just $\text{RO} \cdot \text{U}^2$) and energy. They are extrapolated to Half the time step $T + \text{DT}/2$. (OUTPUT)

GIH - the value of P at $T + \text{DT}/2$

UXN, PXN, GXN, ROXN - values of U, P, G, RO extrapolated to New time $T+DT$, at cell-interface. They are used in CYCEUL to get tentative (pre-monotonized) new cell differences. (OUTPUT)

ZXN, FIH4, ZMDOTL, ZMDOTR - inactive.

A.4 Description of Subroutines

MAIN PROGRAM

The task of this program is to allocate array space for the NMAT arrays required by the present version of GRP code. The length of each array is L . The allocation is done by calling MAIN0. This standard calling sequence is maintained hereafter, thus facilitating modifications.

MAIN0

This subroutine functions as an overall organization routine. It can be read as a kind of flow-chart of the entire computation. First, run set-up is done by calling once to NETUNM (data) and BEGIN (initial conditions). Then a loop over time steps is begun. In each cycle the integration by one time step is performed by calling CYCEUL, and subsequently boundary conditions are implemented by calling SAFAE. Whenever T.EQ.TMUD, results are printed by calling PRINT and TMUD is updated by adding DTMUD.

NETUNM

Here data are set for a particular run. User is invited to modify this routine. There is no input file. This routine is called just once from MAIN0. Note that the detonation data section is skipped when QDET.EQ.0.

BEGIN

Initial conditions are set-up in this routine. The configuration of some nominal case is given in present version. (In CHARGE version it is the detonated spherical charge, using the Taylor self similar solution as initial conditions). User is called to modify this routine so as to generate any other desired initial configuration.

TAYLOR

The purpose of this routine, along with ancillary routines INIDAT, RUNGE and DERIV, is to compute the self-similar Taylor solution [7] of a detonated spherical charge, and implement it as initial conditions for the GRP computation of the ensuing expansion. TAYLOR is called once by BEGIN.

The core of the solution is the numerical (Runge-Kutta) integration of two coupled ordinary differential equations. The integration variable is Ψ . (The flow velocity normalized by DCJ is given

by $U = \text{EXP}(-\text{PSI})$). The two dependent variables are X - the normalized radial coordinate ($X = 1$ at the sphere boundary), and C - the normalized speed of sound. The integration is carried out by calling **RUNGE**, which in turn calls **DERIV** for the evaluation of derivatives. Data for the **TAYLOR** computation is set up by calling (just once) **INIDAT**.

The initial conditions needed in **BEGIN** are values of mass, momentum and (total) energy per cell. These are most accurately computed by spatially integrating the Taylor solution, resulting in lumped mass, momentum and energy per cell, which are then divided by the cell volume. This refinement is significant since gradients are high near the charge boundary ($X = 1$). A total mass and energy check for the entire sphere is performed and printed.

INIDAT, RUNGE, DERIV

Subroutines used only in conjunction with the Taylor initial conditions setup. See **TAYLOR** above.

RATIO, CROSS

User-defined routines. If $A(X)$ is the duct cross-section area, then $\text{CROSS}(X) = A(X)$ and $\text{RATIO}(X) = D[\ln(A(X))]/DX$.

CYCEUL

This is the central computation routine. All major stages of the GRP scheme are performed by calling specific subroutines from **CYCEUL**. Then $RO(I)$, $TENA(I)$ and $E(I)$ are updated to new time $T + DT$ by solving the appropriate conservation laws in **CYCEUL**.

The first loop (DO 1) performs a set of preparatory steps as follows :

- (a) **CALL RIEMAN** - Solving the local Riemann Problem at each $X(I)$.
- (b) **CALL MAGA** - Solving the local Generalized Riemann Problem at each $X(I)$.
- (c) **CALL FLUXE** - Computing second-order fluxes at $X(I)$.
- (d) Evaluation of cell-interface finite differences $DU(I)$, $DP(I)$, $DRO(I)$ in each cell. These will be used at the future time step (after monotonicization) for piecewise-linear interpolation of the flow in each cell. (See definition of $DUDXIL$, $DPDXIL$,..., just preceding the call to **MAGA** in this loop).

Note that in present **CHARGE** version additional computation of **PRESS**, **PULSE1**,..., **PULSE4** has been added. It is just informative and does not interfere in any way with the execution of the

GRP scheme. The purpose of this computation is to monitor the numerical solution and to observe the accuracy within which the asymptotic value of the momentum integral Z (Eq. 2-9 above) is approached.

In the second loop (DO 2), the integration of the three conservation laws is performed, using second-order fluxes that had been computed in loop 1. Flow variables such as $P(I)$ and $U(I)$ are computed in this loop from the conserved variables. The cycle computation is concluded by calling BDOK1 for monotonicization of $DU(I)$, $DP(I)$ and $DRO(I)$.

SAFAE

In this routine user-defined boundary conditions are implemented. Present version (CHARGE) contains rigid wall at the center of the sphere $X(2)=0$, and an "open boundary" at the outer computational zone limit $X(L)$. The rigid wall condition is achieved by setting up a virtual antisymmetric cell next to the boundary cell, so that the solution to the local Riemann Problem will result in a non-moving contact surface ($U_{STAR}=0$). The open boundary is an approximation to an ideally non-reflecting boundary. Here the virtual cell is $I=L$, and the flow in it is defined as a "continuation" of the flow in the adjacent last cell $I=LL$.

BDOK1

Here the tentative cell-interface differences $DV(I)$ are monotonicized according to neighboring average cell values $V(I-1)$, $V(I)$ and $V(I+1)$. The basic idea is that the cell-interface slope $DV(I)$ should have the same sign as the average slope $V(I+1)-V(I-1)$. When $V(I)$ is a local extremum $DV(I)$ is set to zero. Also, the absolute value of $DV(I)$ is constrained so that the jump from a cell-interface value to the adjacent average value $V(I)$, will never be of opposite sign to $DV(I)$.

DCOLE

When COLELA option is used (not in present CHARGE version), the pre-monotonicized slopes are simply the centered difference $(V(I+1)-V(I-1))/2$. Note that even under this option, the monotonicization routine BDOK1 is subsequently called.

PRINT

Printing of results. Reading this routine is self-explanatory. Note some features added for present CHARGE version. User is called to modify this routine to his specific needs.

SOF

Run termination when an error has been detected. ISTOP is an informative index. All printing of relevant information should be done at the calling routine prior to calling SOF. Note that the run is ended in SOF by deliberately causing a system error of computing SQRT(-1). This is done in order to trigger printing of the sequence of calling routines by the operating system.

RIEMAN

Here a single Riemann Problem (RP) is solved by calling RIEMAN from CYCEUL. Referring to Fig. A-2, the RP is solved by finding the point of intersection (USTAR,PSTAR) of Left-propagating and Right-propagating shock/rarefaction adiabats in the (U,P) plane. Prior to the actual computation, the qualitative wave structure is determined. It is characterized by the index NCASE as follows :

NCASE = 1 - Left wave is rarefaction, Right wave is shock.

NCASE = 2 - Both waves are shock.

NCASE = 3 - Left wave is shock, Right wave is rarefaction.

NCASE = 4 - Both waves are rarefaction.

The computation of (USTAR,PSTAR) is coded separately for each case. Newton-Raphson iteration is employed, the first guess being the intersection of the Left and Right rarefaction branches (or their extrapolations), which is done in closed-form. Since in a smooth flow this guess is close to the exact (USTAR,PSTAR), little extra CPU effort is spent on subsequent Newton-Raphson iterations. These are truly needed only in regions of shock wave computation.

The computation in RIEMAN is concluded by computing UW(1),...,UW(5) (UW(6)=infinity). From these wave speeds, the flux index NFLUX that denotes the location of the X-axis on the (X,T) wave diagram of the RP solution (Fig. A-3), is evaluated. It is later needed in subroutine FLUXE.

MAGA

The major purpose of this routine is to compute DUIDT and DPIDT along the contact surface of the RP solution. Since U and P are continuous across the contact, so are their time-derivatives along the contact. Thus, DUIDT and DPIDT are solved from a set of two linear equations. The coefficients of each equation are determined by GRP analysis of the wave on one side. See References 4-6 (particularly Ref. 6) for details.

FLUXE

The major task of this routine is to compute second-order fluxes. This is done in two phases. The first phase is up to statement 9 CONTINUE, where using NFLUX the X-suffixed values of flow variables and their time-derivatives are defined. An X-suffix means that the variable or its time-derivative are related to the line $X = X(I)$ on the (X,T) wave diagram (Fig. A-3). In the second phase, these variables and their time-derivatives are used to extend fluxes at $X(I)$ to Half-time-step (hence the suffix H), i.e. $T + DT/2$. It is these fluxes which are the second-order accurate fluxes for the integration of the conservation laws from T to $T + DT$. Also, cell-interface flow variables (suffix N) are extended to New time level $T + DT$. These are later used in defining cell differences DU(I), DP(I) and DRO(I) in CYCEUL.

A.5 Listing of GRP Code

```

C$OPTIONS LIST
IMPLICIT REAL*8(A-H,O-Z,$)
C PROGRAM GRP - GENERALIZED RIEMANN PROBLEM.
C EXPANSION OF A DETONATED SPHERICAL CHARGE IN VACUUM.
C INITIAL CONDITIONS FROM TAYLOR'S SELF SIMILAR SOLUTION.
COMMON B(102,26)
1 ,ENDB
COMMON /AB/A(50)
EQUIVALENCE (L,A(1)),(LL,A(2)),(T,A(3)),(DT,A(4)),(TMAX,A(5)),
1 (TMUD,A(6)),(DTMUD,A(7)),(JOB,A(8)),(NERI,A(9)),
2 (JJJ,A(10)),(KEYMON,A(11)),(NCYC,A(12))
EQUIVALENCE (COLELA,A(13))
EQUIVALENCE (LAGEUL,A(14))
EQUIVALENCE (UGAL,A(15))
EQUIVALENCE (KEYEK,A(16))
EQUIVALENCE (NCYCPR,A(17))
EQUIVALENCE (STAB,A(18)),(DTBA,A(19)),(DTKOD,A(20)),(KDT,A(21))
COMMON /MONIT/CASEAV(4),NC14(4),NF16(6),
1 NMONU(4),NMONP(4),NMONRO(4),NMONZ(4)
DIMENSION NZERO(26)
EQUIVALENCE (NZERO(1),NC14(1))
COMMON/PULS/PRESS(10),PULSE1(10),PULSE2(10),PULSE3(10),PULSE4(10)
C*****
DO 20 N=1,26
20 NZERO(N)=0
DO 21 N=1,4
21 CASEAV(N)=0.
DO 31 N=1,10
PRESS(N)=0.
PULSE1(N)=0.
PULSE2(N)=0.
PULSE3(N)=0.
PULSE4(N)=0.
31 CONTINUE
NMAT=26
C L=(LOCFC(ENDB)-LOCFC(B(1,1)))/NMAT
L=102
LL=L-1
NN=NMAT*L
DO 1 I=1,L
DO 1 II=1,NMAT
1 B(I,II)=0.
CALL MAINO(L,B(1,1),B(1,2),B(1,3),B(1,4),B(1,5),
1 B(1,6),B(1,7),B(1,8),B(1,9),B(1,10),
2 B(1,11),B(1,12),B(1,13),B(1,14),B(1,15),
3 B(1,16),B(1,17),B(1,18),B(1,19),B(1,20),
4 B(1,21),B(1,22),B(1,23),B(1,24),B(1,25),
5 B(1,26))
STOP
END
SUBROUTINE MAINO
1 (L,X,U,P,RO,G,E,DU,DP,DRO,DG,DXSI,MIN,
2 US,PS,UIDOT,PIDOT,
* FIMZ,ZMDOT,
3 TENA,FIRO,FIM,FIE,GIP,VOL,Z,DZ)
IMPLICIT REAL*8(A-H,O-Z,$)
DIMENSION X(L),U(L),P(L),RO(L),G(L),E(L),DU(L),DP(L),DRO(L),
1 DG(L),DXSI(L),MIN(L),
2 US(L),PS(L),UIDOT(L),PIDOT(L)
3 ,TENA(L),FIRO(L),FIM(L),FIE(L)
4 ,GIP(L),VOL(L),Z(L),DZ(L)
5 ,FIMZ(L),ZMDOT(L)
COMMON /AB/A(50)
EQUIVALENCE (LL,A(2)),(T,A(3)),(DT,A(4)),(TMAX,A(5)),
1 (TMUD,A(6)),(DTMUD,A(7)),(JOB,A(8)),(NERI,A(9)),
2 (JJJ,A(10)),(KEYMON,A(11)),(NCYC,A(12))
EQUIVALENCE (LAGEUL,A(14))
EQUIVALENCE (NCYCPR,A(17))
EQUIVALENCE (STAB,A(18)),(DTBA,A(19)),(DTKOD,A(20)),(KDT,A(21))
COMMON /TOT/AMTOT,ETOT,EKTOT,EPTOT,TENTOT
C*****
T=0.

```

```

NCYC=0
JJJ=0
CALL NETUNM
DELT=DT
CALL BEGIN
1      (L,X,U,P,RO,G,E,DU,DP,DRO,DG,DXSI,MIN,
2      US,PS,UIDOT,PIDOT,
*      FIMZ,ZMDOT,
3      TENA,FIRO,FIM,FIE,GIP,VOL,Z,DZ)
CALL SAFAE
1      (L,X,U,P,RO,G,E,DU,DP,DRO,DG,DXSI,MIN,
2      US,PS,UIDOT,PIDOT,
*      FIMZ,ZMDOT,
3      TENA,FIRO,FIM,FIE,GIP,VOL,Z,DZ)
1      NCYC=NCYC+1
C TIME STEP CONTROL.
DT=DTBA
IF(DT.GT.1.1D0*DTKOD.AND.DTKOD.NE.0.) DT=1.1D0*DTKOD
IF(NCYC.EQ.2) DT=DT/10.D0
IF(NCYC.EQ.1) DT=0.
IF(DT.EQ.0.) GO TO 11
NHAD=((TMUD-T)/DT-1.D-10)
IF(NHAD.GE.10) GO TO 11
DT=(TMUD-T)/DFLOAT(NHAD+1)
11     CONTINUE
T=T+DT
IF((NCYC/NCYCPR)*NCYCPR.NE.NCYC.AND.NCYC.GT.NCYCPR) GO TO 33
PRINT 10, NCYC,T,DT,KDT
10     FORMAT(1X,'NCYC=',I4,3X,'T=',D11.4,3X,'DT=',D11.4,3X,'KDT=',I4)
33     CONTINUE
DTBA=DTMUD
KDT=0
NERI=1
IF(DABS(T-TMUD).LT.1.D-8) NERI=0
CALL CYCEUL
1      (L,X,U,P,RO,G,E,DU,DP,DRO,DG,DXSI,MIN,
2      US,PS,UIDOT,PIDOT,
*      FIMZ,ZMDOT,
3      TENA,FIRO,FIM,FIE,GIP,VOL,Z,DZ)
CALL SAFAE
1      (L,X,U,P,RO,G,E,DU,DP,DRO,DG,DXSI,MIN,
2      US,PS,UIDOT,PIDOT,
*      FIMZ,ZMDOT,
3      TENA,FIRO,FIM,FIE,GIP,VOL,Z,DZ)
IF(NERI.NE.0) GO TO 2
CALL PRINT
1      (L,X,U,P,RO,G,E,DU,DP,DRO,DG,DXSI,MIN,
2      US,PS,UIDOT,PIDOT,
*      FIMZ,ZMDOT,
3      TENA,FIRO,FIM,FIE,GIP,VOL,Z,DZ)
IF(DABS(T-TMUD).LT.1.D-8) TMUD=TMUD+DTMUD
2      CONTINUE
DTKOD=DT
IF(T.LT.TMAX-1.D-8) GO TO 1
RETURN
END
SUBROUTINE NETUNM
IMPLICIT REAL*8(A-H,O-Z,$)
COMMON /AB/A(50)
EQUIVALENCE (L,A(1))
EQUIVALENCE (LL,A(2)),(T,A(3)),(DT,A(4)),(TMAX,A(5)),
1          (TMUD,A(6)),(DTMUD,A(7)),(JOB,A(8)),(NERI,A(9)),
2          (JJJ,A(10)),(KEYMON,A(11)),(NCYC,A(12))
EQUIVALENCE (COLELA,A(13))
EQUIVALENCE (LAGEUL,A(14))
EQUIVALENCE (KEYEK,A(16))
EQUIVALENCE (NCYCPR,A(17))
EQUIVALENCE (STAB,A(18)),(DTBA,A(19)),(DTKOD,A(20)),(KDT,A(21))
COMMON/DETO/QDET,PCJDET,RCJDET,UCJDET,DCJDET,PODET,ROODET,
1          RATE,TEPC
COMMON/DIFFUS/U2,P2,R02,ARW
COMMON /DRAW/GODELX,GODELY,UMIN,UMAX,PMIN,PMAX,ROMIN,ROMAX

```

```

1          , XMIN, XMAX, SMIN, SMAX, IVERSA          CHA0152
COMMON /GAM/GAMA, NG, MU2, G1, G2, G3, G4, G5, G6, G7, G8, G9, G10, G11 CHA0153
1          , G12, G13, G14, G15, G16, G17, G18, G19, G20, G21, G22, G23 CHA0154
2          , G24, G25, G26, G27, G28, G29, G30, G31, G32, G33, G34, G35 CHA0155
REAL*8 NG, MU2 CHA0156
NAMELIST /IN/LIN, GAMA, DT, TMUD, DTMUD, TMAX, CHA0157
1          GODELX, GODELY, UMIN, UMAX, PMIN, PMAX, ROMIN, ROMAX, CHA0158
2          SMIN, SMAX, IVERSA, KEYMON, COLELA, STAB CHA0159
3          , LAGEUL, KEYEK CHA0160
4          , QDET CHA0161
XXXXXXXXXXXXXXXXXXXXXXXXXXXXXXXXXXXXXXXXXXXXXXXXXXXXXXXXXXXXXXXXXXXXXXXXXXXX CHA0162
LIN=L CHA0163
LAGEUL=2 CHA0164
NCYCPR=1 CHA0165
KEYEK=1 CHA0166
TMUD=0. CHA0167
DTMUD=10. D0 CHA0168
TMAX=100. D0 CHA0169
STAB=0. 5D0 CHA0170
DT=1. D-2 CHA0171
KEYMON=1 CHA0172
GAMA=3. D0+1. D-6 CHA0173
QDET=0. 04D0 CHA0174
RATE=0. CHA0175
TEMPC=1. D50 CHA0176
GODELX=16 D0 CHA0177
GODELY=20. D0 CHA0178
IVERSA=100 CHA0179
UMIN=0. CHA0180
UMAX= 1. D0 CHA0181
PMIN=0. CHA0182
PMAX=0. 5D0 CHA0183
ROMIN=0. CHA0184
ROMAX=3. D0 CHA0185
SMIN=0. CHA0186
SMAX=0. 03D0 CHA0187
COLELA=0. CHA0188
READ IN CHA0189
PRINT IN CHA0190
GG=2. D0*GAMA/(GAMA-1. D0) CHA0191
NG=GG CHA0192
CONTINUE CHA0193
MU2=(GAMA-1. D0)/(GAMA+1. D0) CHA0194
G1=GAMA-1. D0 CHA0195
G2=1. D0-MU2 CHA0196
G3=2. D0/(3. D0*GAMA-1. D0) CHA0197
G4=(GAMA+1. D0)/2. D0 CHA0198
G5=0. 5D0*(3. D0*GAMA-1. D0)/(GAMA+1. D0) CHA0199
G6=(GAMA+1. D0)/(2. D0*GAMA) CHA0200
G7=2. D0/(GAMA-1. D0) CHA0201
G8=(GAMA-1. D0)/(2. D0*GAMA) CHA0202
G9=(GAMA+1. D0)/(4. D0*GAMA) CHA0203
G10=1. D0/GAMA CHA0204
G11=(GAMA+1. D0)/4. D0 CHA0205
G12=GAMA/(GAMA-1. D0) CHA0206
G13=0. 5D0*(GAMA-3. D0)/(GAMA+1. D0) CHA0207
G14=0. 5D0*(3. D0*GAMA-5. D0)/(GAMA+1. D0) CHA0208
G15=GAMA*(3. D0*GAMA-1. D0) CHA0209
G16=(GAMA+1. D0)/(2. D0*(GAMA-1. D0)) CHA0210
G17=GAMA+1. D0 CHA0211
G18=GAMA*(GAMA+1. D0)/(3. D0*GAMA-1. D0) CHA0212
G19=(3. D0*GAMA-1. D0)/(GAMA+1. D0) CHA0213
G20=2. D0*(GAMA-1. D0)/(3. D0*GAMA-1. D0)**2 CHA0214
G21=GAMA*(3. D0*GAMA-5. D0)/(3. D0*GAMA-1. D0)**2 CHA0215
GODELX=GODELX/2. 54D0 CHA0216
GODELY=GODELY/2. 54D0 CHA0217
CALL NAMPLT(IVERSA) CHA0218
CALL LIMIT(1000. D0) CHA0219
CALL PLOT(0., 0. 5D0, -3) CHA0220
PODET=0. CHA0221

```

```

ROODET=0.
PCJDET=0.
UCJDET=0.
DCJDET=0.
RCJDET=0.
IF(QDET.LE.0.) GO TO 100
C  DETONATION DATA
QDET=0.04D0
PODET=0.
ROODET=1.8D0
PCJDET=PODET-(GAMA-1.D0)*(-QDET)*ROODET+
1  DSQRT(((GAMA-1.D0)*QDET*ROODET)**2-2.D0*MU2*GAMA*
2  (-QDET)*PODET*ROODET)
RCJDET=ROODET*((GAMA+1.D0)*PCJDET-PODET)/(GAMA*PCJDET)
CCJ=DSQRT(GAMA*PCJDET/RCJDET)
DCJDET=CCJ*RCJDET/ROODET
UCJDET=DCJDET-CCJ
PRINT 101
101  FORMAT(1H1,/,1X,'DETONATION DATA'/)
PRINT 102, QDET,GAMA,TEPC,RATE
102  FORMAT(/1X,'QDET,GAMA,TEMP,RATE=',4D18.8)
PRINT 103, ROODET,PODET
103  FORMAT(/1X,'UNBURNED STATE      ROODET,PODET=',2D18.8)
PRINT 104, DCJDET,PCJDET,RCJDET,UCJDET
104  FORMAT(/1X,'CJ POINT      DCJDET,PCJDET,RCJDET,UCJDET=',4D18.8)
100  CONTINUE
RETURN
END
SUBROUTINE BEGIN
1  (L,X,U,P,RO,G,E,DU,DP,DRO,DG,DXSI,MIN,
2  US,PS,UIDOT,PIDOT,
*  FIMZ,ZMDOT,
3  TENA,FIRO,FIM,FIE,GIP,VOL,Z,DZ)
IMPLICIT REAL*8(A-H,O-Z,$)
DIMENSION X(L),U(L),P(L),RO(L),G(L),E(L),DU(L),DP(L),DRO(L),
1  DG(L),DXSI(L),MIN(L),
2  US(L),PS(L),UIDOT(L),PIDOT(L)
3  ,TENA(L),FIRO(L),FIM(L),FIE(L)
4  ,GIP(L),VOL(L),Z(L),DZ(L)
5  ,FIMZ(L),ZMDOT(L)
COMMON /AB/A(50)
COMMON /GAM/GAMA,NG,MU2,G1,G2,G3,G4,G5,G6,G7,G8,G9,G10,G11
1  ,G12,G13,G14,G15,G16,G17,G18,G19,G20,G21,G22,G23
2  ,G24,G25,G26,G27,G28,G29,G30,G31,G32,G33,G34,G35
REAL*8 NG,MU2
EQUIVALENCE (LL,A(2))
EQUIVALENCE (LAGEUL,A(14))
EQUIVALENCE (UGAL,A(15))
EQUIVALENCE (STAB,A(18)),(DTBA,A(19)),(DTKOD,A(20)),(KDT,A(21))
COMMON/DETO/QDET,PCJDET,RCJDET,UCJDET,DCJDET,PODET,ROODET,
1  RATE,TEPC
COMMON /DRAW/GODELX,GODELY,UMIN,UMAX,PMIN,PMAX,ROMIN,ROMAX
1  ,XMIN,XMAX,SMIN,SMAX,IVERSA
COMMON/GIT/ROLIM,ELIM,XGIT(200),ROGIT(200),ROUGIT(200),EGIT(200)
COMMON /GITN/NP0
LOGICAL CSOF
C*****
DTBA=0.
DTKOD=0.
KDT=0
PO=1.D-9
RH00=1.D-7
UO=UCJDET
UGAL=0.
X0=0.
X1=50.D0
XCHARG=10.D0
XMIN=X0
XMAX=X1
DX=(X1-X0)/(L-2.D0)
DO 1 I=2,L
X(I)=X0+(I-2.D0)*DX

```

CHA0224
CHA0225
CHA0226
CHA0227
CHA0228
CHA0229
CHA0230
CHA0231
CHA0232
CHA0233
CHA0234
CHA0235
CHA0236
CHA0237
CHA0238
CHA0239
CHA0240
CHA0241
CHA0242
CHA0243
CHA0244
CHA0245
CHA0246
CHA0247
CHA0248
CHA0249
CHA0250
CHA0251
CHA0252
CHA0253
CHA0254
CHA0255
CHA0256
CHA0257
CHA0258
CHA0259
CHA0260
CHA0261
CHA0262
CHA0263
CHA0264
CHA0265
CHA0266
CHA0267
CHA0268
CHA0269
CHA0270
CHA0271
CHA0272
CHA0273
CHA0274
CHA0275
CHA0276
CHA0277
CHA0278
CHA0279
CHA0280
CHA0281
CHA0282
CHA0283
CHA0284
CHA0285
CHA0286
CHA0287
CHA0288
CHA0289
CHA0290
CHA0291
CHA0292
CHA0293
CHA0294
CHA0295

BEGIN

	CONTINUE	CHA0296
	X(L)=X1	CHA0297
	U0=U0*CROSS(XCHARG)	CHA0298
	DO 2 I=2,LL	CHA0299
	IF(I.GT.2) U(I)=U0/CROSS(X(I))	CHA0300
	P(I)=P0	CHA0301
	RO(I)=RH00	CHA0302
	Z(I)=0.	CHA0303
	GO TO (31,32), LAGEUL	CHA0304
1	CONTINUE	CHA0305
	E(I)=P(I)/((GAMA-1.D0)*RO(I))+0.5D0*U(I)**2+Z(I)*QDET	CHA0306
	GO TO 30	CHA0307
2	CONTINUE	CHA0308
	E(I)=P(I)/(GAMA-1.D0)+0.5D0*RO(I)*U(I)**2+Z(I)*RO(I)*QDET	CHA0309
0	CONTINUE	CHA0310
	G(I)=DSQRT(GAMA*P(I)*RO(I))	CHA0311
	CONTINUE	CHA0312
	DO 3 I=2,LL	CHA0313
	TENA(I)=RO(I)*U(I)	CHA0314
	VOL(I)=(X(I+1)-X(I))*(X(I+1)**2+X(I+1)*X(I)+X(I)**2)/3.D0	CHA0315
	CONTINUE	CHA0316
	INSERT DETONATED CHARGE FLOW FIELD FROM TAYLOR'S SOLUTION.	CHA0317
	CALL TAYLOR(GAMA)	CHA0318
	RONORM=RCJDET	CHA0319
	RUNORM=RCJDET*UCJDET	CHA0320
	ENORM=RCJDET*DCJDET**2	CHA0321
	XLIM=XGIT(NP0)	CHA0322
	NGIT=NP0-1	CHA0323
	XG1=XLIM	CHA0324
	XG2=XGIT(NGIT)	CHA0325
	AROIP =ROGIT (NP0)+ROLIM*XLIM**3/3.D0	CHA0326
	AROUIP=ROUGIT(NP0)	CHA0327
	AEIP =EGIT (NP0)+ ELIM*XLIM**3/3.D0	CHA0328
	XP=X(2)/XCHARG	CHA0329
	DO 100 I=2,LL	CHA0330
	IP=I+1	CHA0331
	XI=XP	CHA0332
	AROIP =AROIP	CHA0333
	AROUIP=AROUIP	CHA0334
	AEI =AEIP	CHA0335
	XP=X(IP)/XCHARG	CHA0336
	IF(DABS(XP-1.D0).LT.1.D-10) XP=1.D0	CHA0337
	CSOF=(XP.GE.1.D0)	CHA0338
	IF(XP.GE.XLIM) GO TO 101	CHA0339
UNI	FORM FLOW REGION	CHA0340
	DELVOL=(XLIM-XP)*(XLIM**2+XLIM*XP+XP**2)/3.D0	CHA0341
	AROIP =ROGIT (NP0)+ROLIM*DELVOL	CHA0342
	AROUIP=ROUGIT(NP0)	CHA0343
	AEIP =EGIT (NP0)+ ELIM*DELVOL	CHA0344
	GO TO 102	CHA0345
01	CONTINUE	CHA0346
	NON UNIFORM FLOW REGION.	CHA0347
	IF(.NOT.CSOF) GO TO 104	CHA0348
	LAST POINT. (THIS IS THE DETONATION FRONT POINT X=1).	CHA0349
	AROIP= 0.	CHA0350
	AROUIP=0.	CHA0351
	AEIP= 0.	CHA0352
	GO TO 102	CHA0353
04	CONTINUE	CHA0354
	IF(XP.LE.XG2) GO TO 103	CHA0355
	NGIT=NGIT-1	CHA0356
	IF(NGIT.LE.0) CALL SOF('BEGIN 104. NGIT.LE.0.')	CHA0357
	XG1=XG2	CHA0358
	XG2=XGIT(NGIT)	CHA0359
	GO TO 104	CHA0360
03	CONTINUE	CHA0361
	FRAC=(XP-XG1)/(XG2-XG1)	CHA0362
	IF(FRAC.LT.0.) CALL SOF('BEGIN 103. FRAC.LT.0.')	CHA0363
	IF(FRAC.GT.1.D0) CALL SOF('BEGIN 103. FRAC.GT.1.')	CHA0364
	AROIP =(1.D0-FRAC)*ROGIT (NGIT+1)+FRAC*ROGIT (NGIT)	CHA0365
		CHA0367

```

        AROUIP=(1.D0-FRAC)*ROUGIT(NGIT+1)+FRAC*ROUGIT(NGIT)
        AEIP =(1.D0-FRAC)*EGIT (NGIT+1)+FRAC*EGIT (NGIT)
102 CONTINUE
C COMPUTE MASS, MOMENTUM AND ENERGY DENSITIES.
  IF(XP.LE.XLIM) GO TO 105
C CONSERVATION-FORM DEFINITION OF MASS, MOMENTUM AND ENERGY DENSITY.
  DVOL=(XP-XI)*(XP**2+XP*XI+XI**2)/3.D0
  RO (I)=RONORM*(AROI - AROIP)/DVOL
  TENA(I)=RUNORM*(AROI-AROUIP)/DVOL
  E (I)=ENORM *(AEI - AEIP)/DVOL
  GO TO 106
105 CONTINUE
C UNIFORM FLOW REGION
  RO (I)=RONORM*ROLIM
  TENA(I)=0.
  E (I)=ENORM * ELIM
106 CONTINUE
  U(I)=TENA(I)/RO(I)
  P(I)=(GAMA-1.D0)*(E(I)-0.5D0*RO(I)*U(I)**2)
  PRINT 111,I,CSOF,U(I),P(I),RO(I),E(I)
111 FORMAT(1X,'I,CSOF,U,P,RO,E=',I4,L3,4D14.4)
  IF(CSOF) GO TO 109
100 CONTINUE
109 CONTINUE
  DO 4 I=2,LL
  DXSI(I)=(X(I+1)-X(I))*RO(I)
  4 CONTINUE
  RETURN
  END
SUBROUTINE TAYLOR(GAMA)
  IMPLICIT REAL*8(A-H,O-Z,$)
TAYLOR
C
C TAYLOR -- SELF SIMILAR SPHERICAL DETONATION (CJ) FLOW FIELD
C
  COMMON /GGGG/G,G1,G2,G3,G4,G5,G6,G7,G8,G9,G10
  COMMON /PAR/RH00,Q0,ROCJ,DCJ,UCJ,PCJ,DPSI,PSIMAX,C0,U0
  COMMON /GIT/NP0
  COMMON/GIT/ROLIM,ELIM,XGIT(200),ROGIT(200),ROUGIT(200),EGIT(200)
C*****
G=GAMA
  PRINT 101
101 FORMAT('1')
  PRINT 110
110 FORMAT(1X,'G. I. TAYLOR SOLUTION. N,PSI,U,C,X/AM,AT,AE='//)
  CALL INIDAT
  X=1.D0
  Y=0.
  U=U0
  C=C0
  AM=0.
  AT=0.
  AE=0.
  PSI=-DLOG(U)
  DO 1 N=1,NP0
  XGIT (N)=X
  ROGIT (N)=AM
  ROUGIT(N)=AT
  EGIT (N)=AE
  PRINT 11,N,PSI,U,C,X,AM,AT,AE
11 FORMAT(1X,I4,4D14.5/5X,3D14.5)
  CALL RUNGE(N,PSI,X,C,AM,AT,AE,PSIN,XN,CN,AMN,ATN,AEN)
  PSI=PSIN
  U=DEXP(-PSI)
  X=XN
  C=CN
  AM=AMN
  AT=ATN
  AE=AEN
1 CONTINUE
  ROLIM=(C/C0)**G3
  ELIM=G5*(C/C0)**G4
  AM0=AM+(C/C0)**G3*X**3/3.D0

```

```

AM0=AM0*3.D0*(G+1.D0)/G
AE0=AE+(G5*(C/C0)**G4+0.5D0*(C/C0)**G3*U**2)*X**3/3.D0
AE0=AE0*6.D0*(G+1.D0)*(G**2-1.D0)/G
PRINT 22,AM0,AE0
2 FORMAT(///1X,'MASS AND ENERGY CHECK (SHOULD BE 1.)'///
1 1X,'M0=',D17.8,5X,'E0=',D17.8//)
RETURN
END

```

CHA0440
CHA0441
CHA0442
CHA0443
CHA0444
CHA0445
CHA0446
CHA0447

```

SUBROUTINE INIDAT
IMPLICIT REAL*8(A-H,O-Z,$)
COMMON /GGGG/G,G1,G2,G3,G4,G5,G6,G7,G8,G9,G10
COMMON /PAR/RH00,Q0,ROCJ,DCJ,UCJ,PCJ,DPSI,PSIMAX,C0,U0
COMMON /GITN/NP0

```

INIDAT

CHA0448
CHA0449
CHA0450
CHA0451
CHA0452

```

*****
NP0=200
PSIMAX=10.D0
U0=1.D0/(G+1.D0)
C0=1.D0-U0
DPSI=PSIMAX/DFLOAT(NP0)
G1=G-1.D0
G2=G1/2.D0
G3=2.D0/(G-1.D0)
G4=2.D0*G/(G-1.D0)
G5=G/((G+1.D0)**2*(G-1.D0))
RETURN
END

```

RUNGE

CHA0453
CHA0454
CHA0455
CHA0456
CHA0457
CHA0458
CHA0459
CHA0460
CHA0461
CHA0462
CHA0463
CHA0464
CHA0465

```

SUBROUTINE RUNGE(N,PSI,X,C,AM,AT,AE,PSIN,XN,CN,AMN,ATN,AEN)
IMPLICIT REAL*8(A-H,O-Z,$)
COMMON /GGGG/G,G1,G2,G3,G4,G5,G6,G7,G8,G9,G10
COMMON /PAR/RH00,Q0,ROCJ,DCJ,UCJ,PCJ,DPSI,PSIMAX,C0,U0
COMMON /GITN/NP0

```

```

*****
H=DPSI
H2=H/2.D0
H6=H/6.D0
CALL DERIV(PSI,X,C,AM,AT,AE,
1 DXDP1,DCDP1,DMDP1,DTDP1,DEDP1)
CALL DERIV(PSI+H2,X+H2*DXDP1,C+H2*DCDP1,AM,AT,AE,
1 DXDP2,DCDP2,DMDP2,DTDP2,DEDP2)
CALL DERIV(PSI+H2,X+H2*DXDP2,C+H2*DCDP2,AM,AT,AE,
1 DXDP3,DCDP3,DMDP3,DTDP3,DEDP3)
CALL DERIV(PSI+H,X+H*DXDP3,C+H*DCDP3,AM,AT,AE,
1 DXDP4,DCDP4,DMDP4,DTDP4,DEDP4)
PSIN=PSI+H
XN=X+H6*(DXDP1+2.D0*(DXDP2+DXDP3)+DXDP4)
CN=C+H6*(DCDP1+2.D0*(DCDP2+DCDP3)+DCDP4)
AMN=AM+H6*(DMDP1+2.D0*(DMDP2+DMDP3)+DMDP4)
ATN=AT+H6*(DTDP1+2.D0*(DTDP2+DTDP3)+DTDP4)
AEN=AE+H6*(DEDP1+2.D0*(DEDP2+DEDP3)+DEDP4)
RETURN
END

```

DERIV

CHA0471
CHA0472
CHA0473
CHA0474
CHA0475
CHA0476
CHA0477
CHA0478
CHA0479
CHA0480
CHA0481
CHA0482
CHA0483
CHA0484
CHA0485
CHA0486
CHA0487
CHA0488
CHA0489
CHA0490

```

SUBROUTINE DERIV(PSI,X,C,AM,AT,AE,DXDP,DCDP,DMDP,DTDP,DEDP)
IMPLICIT REAL*8(A-H,O-Z,$)
COMMON /GGGG/G,G1,G2,G3,G4,G5,G6,G7,G8,G9,G10
COMMON /PAR/RH00,Q0,ROCJ,DCJ,UCJ,PCJ,DPSI,PSIMAX,C0,U0
COMMON /GITN/NP0

```

```

*****
U=DEXP(-PSI)
DXDP=0.5D0*X*(C-U+X)*(C+U-X)/C**2
DCDP=-G2*U*(X-U)/C
DMDP=-(C/C0)**G3*X**2*DXDP
DTDP=DMDP*U
DEDP=-(G5*(C/C0)**G4+0.5D0*(C/C0)**G3*U**2)*X**2*DXDP
RETURN
END

```

RATIO

CHA0491
CHA0492
CHA0493
CHA0494
CHA0495
CHA0496
CHA0497
CHA0498
CHA0499
CHA0500
CHA0501
CHA0502
CHA0503
CHA0504

```

DOUBLE PRECISION FUNCTION RATIO(X)
IMPLICIT REAL*8(A-H,O-Z,$)
*****
RATIO=0.
IF(X.LE.1.D-8)RETURN
RATIO=2.D0/X
RETURN

```

CHA0505
CHA0506
CHA0507
CHA0508
CHA0509
CHA0510
CHA0511

	END		CHA0512
	DOUBLE PRECISION FUNCTION CROSS(X)	CROSS	CHA0513
	IMPLICIT REAL*8(A-H,O-Z,\$)		CHA0514
C*****	*****		CHA0515
C	CROSS=1.DO		CHA0516
	CROSS=X**2		CHA0517
	RETURN		CHA0518
	END		CHA0519
	SUBROUTINE CYCEUL	CYCEUL	CHA0520
1	(L,X,U,P,RO,G,E,DU,DP,DRO,DG,DXSI,MIN,		CHA0521
2	US,PS,UIDOT,PIDOT,		CHA0522
*	FIMZ,ZMDOT,		CHA0523
3	TENA,FIRO,FIM,FIE,GIP,VOL,Z,DZ)		CHA0524
	IMPLICIT REAL*8(A-H,O-Z,\$)		CHA0525
	DIMENSION X(L),U(L),P(L),RO(L),G(L),E(L),DU(L),DP(L),DRO(L),		CHA0526
1	DG(L),DXSI(L),MIN(L),		CHA0527
2	US(L),PS(L),UIDOT(L),PIDOT(L)		CHA0528
3	,TENA(L),FIRO(L),FIM(L),FIE(L)		CHA0529
4	,GIP(L),VOL(L),Z(L),DZ(L)		CHA0530
5	,FIMZ(L),ZMDOT(L)		CHA0531
	COMMON /AB/A(50)		CHA0532
	EQUIVALENCE (LL,A(2)),(T,A(3)),(DT,A(4)),(COLELA,A(13))		CHA0533
	EQUIVALENCE (KEYEK,A(16))		CHA0534
	EQUIVALENCE (STAB,A(18)),(DTBA,A(19)),(DTKOD,A(20)),(KDT,A(21))		CHA0535
	COMMON /GAM/GAMA,NG,MU2,G1,G2,G3,G4,G5,G6,G7,G8,G9,G10,G11		CHA0536
1	,G12,G13,G14,G15,G16,G17,G18,G19,G20,G21,G22,G23		CHA0537
2	,G24,G25,G26,G27,G28,G29,G30,G31,G32,G33,G34,G35		CHA0538
	REAL*8 NG,MU2		CHA0539
	COMMON /TOT/AMTOT,ETOT,EKTOT,EPTOT,TENTOT		CHA0540
	COMMON /AZOV/ISAF,NORIMN,USAF,PSAF,ROSAF,GSAF,ESAF,DPSAF		CHA0541
1	,DXSIL,DXSIR		CHA0542
	LOGICAL NORIMN		CHA0543
	COMMON /STEP0/UL,PL,ROL,GL,UR,PR,ROR,GR,USTAR,PSTAR,		CHA0544
1	RSTARL,RSTARR,GSTARL,GSTARR,		CHA0545
2	CL,CR,CSTARL,CSTARR,SL,SR,WL,WR,UW(6)		CHA0546
3	,LAMDAL,LAMDAR,RATEL,RATER,TEMPL,TEMPSL,TEMPSR		CHA0547
4	,ZL,ZR,ZSTARL,ZSTARR,NFLUX,HELEML,HELEMR		CHA0548
	REAL*8 LAMDAL,LAMDAR		CHA0549
	LOGICAL HELEML,HELEMR		CHA0550
	COMMON /STEP1/DUIDT,DPIDT,DGIDTL,DGIDTR,DRIDTL,DRIDTR		CHA0551
2	,ASTARL,ASTARR,LAMDSL,LAMDSR,DSDAL,DSDAR,DZDAL,DZDAR		CHA0552
3	,RAT,SH		CHA0553
4	,BETACL,BETACR,DSDASL,DSDASR,DZDASL,DZDASR		CHA0554
	REAL*8 LAMDSL,LAMDSR,DSDAL,DSDAR,DZDAL,DZDAR		CHA0555
	COMMON /GRADS/DUDXIL,DPDXIL,DGDIXIL,DRDXIL,DZDXIL,DSDXIL,		CHA0556
1	DUDXIR,DPDXIR,DGDIXIR,DRDXIR,DZDXIR,DSDXIR		CHA0557
	COMMON /FI/FIH1,FIH2,FIH3,UXN,PXN,GXN,ROXN,ZXN		CHA0558
1	,GIH		CHA0559
2	,FIH4,ZMDOTL,ZMDOTR		CHA0560
	COMMON/DETO/QDET,PCJDET,RCJDET,UCJDET,DCJDET,PODET,ROODET,		CHA0561
1	RATE,TEMPC		CHA0562
	COMMON/PULS/PRESS(10),PULSE1(10),PULSE2(10),PULSE3(10),PULSE4(10)		CHA0563
	DATA ERRP/0.DO/		CHA0564
	DATA NERRP/0/		CHA0565
C	DATA KOTZ/7777777777B/		CHA0566
C*****	*****		CHA0567
	DT2=DT/2.DO		CHA0568
	UXN=0.		CHA0573
	PXN=0.		CHA0574
	ROXN=0.		CHA0575
	ZXN=0.		CHA0576
	DO 1 I=2,L		CHA0577
	IM=I-1		CHA0578
	UXNM=UXN		CHA0579
	PXNM=PXN		CHA0580
	ROXNM=ROXN		CHA0581
	ZXNM=ZXN		CHA0582
	UL=U(IM)+0.5DO*DU(IM)		CHA0583
	PL=P(IM)+0.5DO*DP(IM)		CHA0584
	ROL=RO(IM)+0.5DO*DRO(IM)		CHA0585
	GL=DSQRT(GAMA*PL*ROL)		CHA0586
	CL=GL/ROL		CHA0587

```

ZL=Z(IM)+0.5D0*DZ(IM)
IF(ZL.GT.1.D0) ZL=1.D0
IF(ZL.LT.0. ) ZL=0.
SL=PL/(G1*ROL**GAMA)
TEMPL=PL/ROL
UR=U(I)-0.5D0*DU(I)
PR=P(I)-0.5D0*DP(I)
ROR=RO(I)-0.5D0*DRO(I)
GR=DSQRT(GAMA*PR*ROR)
CR=GR/ROR
ZR=Z(I)-0.5D0*DZ(I)
IF(ZR.GT.1.D0) ZR=1.D0
IF(ZR.LT.0. ) ZR=0.
SR=PR/(G1*ROR**GAMA)
TEMPR=PR/ROR

CALL RIEMAN(L,I,MIN)

DUDXIL=DU(IM)/DXSI(IM)
DPDXIL=DP(IM)/DXSI(IM)
DRDXIL=DRO(IM)/DXSI(IM)
DGDIXIL=0.5D0*GL*(DPDXIL/PL+DRDXIL/ROL)
DZDXIL=DZ(IM)/DXSI(IM)
DSDXIL=SL*(DPDXIL/PL-GAMA*DRDXIL/ROL)
DUDXIR=DU(I)/DXSI(I)
DPDXIR=DP(I)/DXSI(I)
DRDXIR=DRO(I)/DXSI(I)
DGDIXIR=0.5D0*GR*(DPDXIR/PR+DRDXIR/ROR)
DZDXIR=DZ(I)/DXSI(I)
DSDXIR=SR*(DPDXIR/PR-GAMA*DRDXIR/ROR)
SH=CROSS(X(I))
RAT=RATIO(X(I))

CALL MAGA(L,I,MIN)

US(I)=USTAR
PS(I)=PSTAR
UIDOT(I)=DUIDT
PIDOT(I)=DPIDT

CALL FLUXE(L,I,MIN)

FIRO(I)=FIH1
FIM(I)=FIH2
FIE(I)=FIH3
FIMZ(I)=FIH4
GIP(I)=GIH
DU(IM)=UXN-UXNM
DP(IM)=PXN-PXNM
DRO(IM)=ROXN-ROXNM
DZ(IM)=ZXM-ZXNM
STATIONS OUTPUT
IF((I-42)*(I-62)*(I-82)*(I-102).NE.0) GO TO 1
NPU=0
IF(I.EQ.42) NPU=1
IF(I.EQ.62) NPU=2
IF(I.EQ.82) NPU=3
IF(I.EQ.102)NPU=4
IF(NPU.EQ.0) CALL SOF('FLUXE 90. NPU.EQ.0')
PRESS(NPU)=GIH+FIH2
PULSE1(NPU)=PULSE1(NPU)+DT*GIH
PULSE2(NPU)=PULSE2(NPU)+DT*(GIH+FIH2)
PULSE3(NPU)=PULSE3(NPU)+DT*FIH1*CROSS(X(I))
PULSE4(NPU)=PULSE4(NPU)+DT*FIH2*CROSS(X(I))
CONTINUE

AMTOT=0.
ETOT=0.
EKTOT=0.
EPTOT=0.
TENTOT=0.
FI1=FIRO(2)

```

```

CHA0588
CHA0589
CHA0590
CHA0591
CHA0592
CHA0593
CHA0594
CHA0595
CHA0596
CHA0597
CHA0598
CHA0599
CHA0600
CHA0601
CHA0602
CHA0603
CHA0604
CHA0605
CHA0606
CHA0607
CHA0608
CHA0609
CHA0610
CHA0611
CHA0612
CHA0613
CHA0614
CHA0615
CHA0616
CHA0617
CHA0618
CHA0619
CHA0620
CHA0621
CHA0622
CHA0623
CHA0624
CHA0625
CHA0626
CHA0627
CHA0628
CHA0629
CHA0630
CHA0631
CHA0632
CHA0633
CHA0634
CHA0635
CHA0636
CHA0637
CHA0638
CHA0639
CHA0640
CHA0641
CHA0642
CHA0643
CHA0644
CHA0645
CHA0646
CHA0647
CHA0648
CHA0649
CHA0650
CHA0651
CHA0652
CHA0653
CHA0654
CHA0655
CHA0656
CHA0657
CHA0658
CHA0659

```

	FI2=FIM (2)	CHA0660
	FI3=FIE (2)	CHA0661
	FI4=FIMZ(2)	CHA0662
	GI2=GIP(2)	CHA0663
	SH=CROSS(X(2))	CHA0664
	DO 2 I=2,LL	CHA0665
	IP=I+1	CHA0666
	FIM1=FI1	CHA0667
	FIM2=FI2	CHA0668
	FIM3=FI3	CHA0669
	FIM4=FI4	CHA0670
	GIM2=GI2	CHA0671
	SHM=SH	CHA0672
	FI1=FI0(IP)	CHA0673
	FI2=FIM (IP)	CHA0674
	FI3=FIE (IP)	CHA0675
	FI4=FIMZ(IP)	CHA0676
	GI2=GIP (IP)	CHA0677
	SH=CROSS(X(IP))	CHA0678
	DVOL=VOL(I)	CHA0679
	ROOLD=RO(I)	CHA0680
	POLD=P(I)	CHA0681
	EOLD=E(I)	CHA0682
	UOLD=U(I)	CHA0683
	ZOLD=Z(I)	CHA0684
	ZKODM=ZOLD*ROOLD	CHA0685
	TOLD=POLD/ROOLD	CHA0686
	DX=X(IP)-X(I)	CHA0687
	DTVOL=DT/DVOL	CHA0688
C		CHA0689
	RO(I)=RO(I)-DTVOL*(SH*FI1-SHM*FIM1)	CHA0690
	TENA(I)=TENA(I)-DTVOL*(SH*FI2-SHM*FIM2)-(DT/DX)*(GI2-GIM2)	CHA0691
	E(I)=E(I)-DTVOL*(SH*FI3-SHM*FIM3)	CHA0692
	U(I)=TENA(I)/RO(I)	CHA0693
	Z(I)=(ZKODM-DTVOL*(SH*FI4-SHM*FIM4))/RO(I)	CHA0694
	IF(Z(I).GT.1.D0) Z(I)=1.D0	CHA0695
	IF(Z(I).LT.0.) Z(I)=0.	CHA0696
C		CHA0697
	UAV=U(I)	CHA0698
	ROAV=RO(I)	CHA0699
	EP=E(I)-0.5D0*ROAV*UAV**2	CHA0700
	IF(EP.GT.0.) GO TO 291	CHA0701
	NERRP=NERRP+1	CHA0702
	ERRP=ERRP+(1.D-8-EP)*DVOL	CHA0703
	IF(ERRP.GT.0.24D0) GO TO 291	CHA0704
	EP=1.D-8	CHA0705
291	CONTINUE	CHA0706
	IF(EP.LE.0.) GO TO 7001	CHA0707
	P(I)=G1*EP	CHA0708
	G(I)=DSQRT(GAMA*P(I)*RO(I))	CHA0709
C		CHA0710
	UPC=DABS(U(I))+G(I)/RO(I)	CHA0711
	DTI=STAB*DX/UPC	CHA0712
	IF(DTI.GT.DTBA) GO TO 29	CHA0713
	DTBA=DTI	CHA0714
	KDT=I	CHA0715
29	CONTINUE	CHA0716
	DXSI(I)=RO(I)*DX	CHA0717
	ETOT=ETOT+E(I)*DVOL	CHA0718
	EPTOT=EPTOT+EP*DVOL	CHA0719
	AMTOT=AMTOT+RO(I)*DVOL	CHA0720
	TENTOT=TENTOT+TENA(I)*DVOL	CHA0721
2	CONTINUE	CHA0722
	EKTOT=ETOT-EPTOT	CHA0723
C		CHA0724
	IF(COLELA.EQ.0.) GO TO 200	CHA0725
	CALL DCOLE(L,X,U ,DU ,MIN,1)	CHA0726
	CALL DCOLE(L,X,P,DP,MIN,2)	CHA0727
	CALL DCOLE(L,X,RO,DRO,MIN,3)	CHA0728
	CALL DCOLE(L,X,Z,DZ,MIN,4)	CHA0729
200	CONTINUE	CHA0730
	CALL BDOK1(L,X,U ,DU ,MIN,1)	CHA0731

```

CALL BDOK1(L,X,P,DP,MIN,2)
CALL BDOK1(L,X,RO,DRO,MIN,3)
CALL BDOK1(L,X,Z,DZ,MIN,4)
PRINT 901,(NN,PRESS(NN),PULSE1(NN),PULSE2(NN),
1 PULSE3(NN)/AMTOT,PULSE4(NN)/TENTOT,NN=1,4)
01 FORMAT(1X,2(' / ',I3,5D11.3,' / ')/)
IF(DABS(T-A(5)).LT.1.D-6) PRINT 911,NERRP,ERRP
11 FORMAT(/1X,'NERRP,ERRP=',I5,D15.5/)
RETURN
001 CONTINUE
PRINT 7101,I,ROAV,UAV,DRO(I),DU(I),E(I),EP,ZNEW,ZNEW-1.DO,EPI
101 FORMAT(/1X,'FROM CYCEUL. NEGATIVE EP. IN CELL I=',I6//
1 1X,'ROAV,UAV,DRO(I),DU(I)=' ,4D18.8//
2 1X,'E(I),EP,ZNEW,ZNEW-1,EPI=' ,5D14.6//)
CALL PRINT
1 (L,X,U,P,RO,G,E,DU,DP,DRO,DG,DXSI,MIN,
2 US,PS,UIDOT,PIDOT,
* FIMZ,ZMDOT,
3 TENA,FIRO,FIM,FIE,GIP,VOL,Z,DZ)
CALL SOF('CYCEUL 7001, NEGATIVE EP')
RETURN
END
SUBROUTINE SAFAE SAFAE
1 (L,X,U,P,RO,G,E,DU,DP,DRO,DG,DXSI,MIN,
2 US,PS,UIDOT,PIDOT,
* FIMZ,ZMDOT,
3 TENA,FIRO,FIM,FIE,GIP,VOL,Z,DZ)
IMPLICIT REAL*8(A-H,O-Z,$)
DIMENSION X(L),U(L),P(L),RO(L),G(L),E(L),DU(L),DP(L),DRO(L),
1 DG(L),DXSI(L),MIN(L),
2 US(L),PS(L),UIDOT(L),PIDOT(L)
3 ,TENA(L),FIRO(L),FIM(L),FIE(L)
4 ,GIP(L),VOL(L),Z(L),DZ(L)
5 ,FIMZ(L),ZMDOT(L)
COMMON /AB/A(50)
EQUIVALENCE (LL,A(2)),(T,A(3)),(DT,A(4)),(NCYC,A(12))
EQUIVALENCE (UGAL,A(15))
COMMON /GAM/GAMA,NG,MU2,G1,G2,G3,G4,G5,G6,G7,G8,G9,G10,G11
1 ,G12,G13,G14,G15,G16,G17,G18,G19,G20,G21,G22,G23
2 ,G24,G25,G26,G27,G28,G29,G30,G31,G32,G33,G34,G35
REAL*8 NG,MU2
COMMON/DETO/QDET,PCJDET,RCJDET,UCJDET,DCJDET,PODET,ROODET,
1 RATE,TEMPC
COMMON/DIFFUS/U2,P2,RO2,ARW
*****
RIGID B.C. AT I=2
U(1)=-U(2)
P(1)=P(2)
G(1)=G(2)
RO(1)=RO(2)
Z(1)=Z(2)
DU(1)=DU(2)
DP(1)=-DP(2)
DG(1)=-DG(2)
DRO(1)=-DRO(2)
DXSI(1)=DXSI(2)

OUTFLOW B.C. AT I=L
U(L)=U(LL)+DU(LL)/2.DO
P(L)=P(LL)+DP(LL)/2.DO
RO(L)=RO(LL)+DRO(LL)/2.DO
G(L)=G(LL)+DG(LL)/2.DO
Z(L)=Z(LL)+DZ(LL)/2.DO
DU(L)=0.
DP(L)=0.
DG(L)=0.
DRO(L)=0.
DZ(L)=0.
DXSI(L)=DXSI(LL)

```

C

	RETURN	CHA0804
	END	CHA0805
	SUBROUTINE BDOK1(L,X,V,DV,MIN,NV)	CHA0806
	IMPLICIT REAL*8(A-H,O-Z,\$)	BDOK1
	DIMENSION X(L),V(L),DV(L),MIN(L)	CHA0807
	COMMON /AB/A(50)	CHA0808
	EQUIVALENCE (LL,A(2)),(KEYMON,A(11))	CHA0809
	COMMON /DRAW/GODELX,GODELY,UMIN,UMAX,PMIN,PMAX,ROMIN,ROMAX	CHA0810
1	,XMIN,XMAX,SMIN,SMAX,IVERSA	CHA0811
1	COMMON /MONIT/CASEAV(4),NC14(4),NF16(6),	CHA0812
	NMONU(4),NMONP(4),NMONRO(4),NMONZ(4)	CHA0813
	DIMENSION NMONV(4,4)	CHA0814
	EQUIVALENCE (NMONV(1,1),NMONU(1))	CHA0815
	DIMENSION NAMEV(4)	CHA0816
	DATA NAMEV/'U','P','RO','Z' /	CHA0817
	DATA EPS/1.D-9 /	CHA0818
C*****		CHA0819
	GO TO (1,2,3,4), NV	CHA0820
1	AMIDA=(UMAX-UMIN)**2	CHA0821
	GO TO 9	CHA0822
2	AMIDA=(PMAX-PMIN)**2	CHA0823
	GO TO 9	CHA0824
3	AMIDA=(ROMAX-ROMIN)**2	CHA0825
	GO TO 9	CHA0826
4	AMIDA=1.D0	CHA0827
	GO TO 9	CHA0828
9	CONTINUE	CHA0829
	AMIDA=AMIDA*EPS**2	CHA0830
	EPSA=DSQRT(AMIDA)	CHA0831
	DO 29 I=2,LL	CHA0832
	ICAT=0	CHA0833
	IF(DABS(DV(I)).LE.EPSA) DV(I)=0.	CHA0834
	IF(DV(I).EQ.0.) GO TO 29	CHA0835
	VLEFT=V(I)-0.5D0*DV(I)	CHA0836
	VRIGHT=V(I)+0.5D0*DV(I)	CHA0837
	VM=V(I-1)	CHA0838
	VP=V(I+1)	CHA0839
	SIGN=(VP-V(I))*(V(I)-VM)	CHA0840
	IF(SIGN.GT.-AMIDA) GO TO 22	CHA0841
21	DV(I)=0.	CHA0842
	ICAT=1	CHA0843
	GO TO 20	CHA0844
22	CONTINUE	CHA0845
	SIGN=(VP-VM)*DV(I)	CHA0846
	IF(SIGN.GT.-AMIDA) GO TO 24	CHA0847
23	DV(I)=0.5D0*(VP-VM)	CHA0848
	VLEFT=V(I)-0.5D0*DV(I)	CHA0849
	VRIGHT=V(I)+0.5D0*DV(I)	CHA0850
	ICAT=2	CHA0851
24	SIGN=(VLEFT-VM)*DV(I)	CHA0852
	IF(SIGN.GT.-AMIDA) GO TO 26	CHA0853
25	VLEFT=VM	CHA0854
	VRIGHT=2.D0*V(I)-VLEFT	CHA0855
	DV(I)=VRIGHT-VLEFT	CHA0856
	ICAT=3	CHA0857
26	SIGN=(VP-VRIGHT)*DV(I)	CHA0858
	IF(SIGN.GT.-AMIDA) GO TO 28	CHA0859
27	VRIGHT=VP	CHA0860
	VLEFT=2.D0*V(I)-VRIGHT	CHA0861
	DV(I)=VRIGHT-VLEFT	CHA0862
	ICAT=3	CHA0863
28	IF(DABS(DV(I)).LE.0.5D0*DABS(VP-VM)) GO TO 31	CHA0864
30	DV(I)=0.5D0*(VP-VM)	CHA0865
	ICAT=4	CHA0866
31	CONTINUE	CHA0867
20	CONTINUE	CHA0868
	IF(DABS(DV(I)).GT.EPSA) GO TO 40	CHA0869
	DV(I)=0.	CHA0870
40	CONTINUE	CHA0871
	IF(ICAT.GT.0) NMONV(ICAT,NV)=NMONV(ICAT,NV)+1	CHA0872
29	CONTINUE	CHA0873
		CHA0874
		CHA0875


```

RETURN
END
SUBROUTINE DCOLE(L,X,V,DV,MIN,NV)
IMPLICIT REAL*8(A-H,O-Z,$)
DIMENSION X(L),V(L),DV(L),MIN(L)
COMMON /AB/A(50)
EQUIVALENCE (LL,A(2))
*****
DO 1 I=2,LL
IM=I-1
IP=I+1
DV(I)=0.5D0*(V(IP)-V(IM))
CONTINUE
RETURN
END
SUBROUTINE PRINT
(L,X,U,P,RO,G,E,DU,DP,DRO,DG,DXSI,MIN,
US,PS,UIDOT,PIDOT,
FIMZ,ZMDOT,
TENA,FIRO,FIM,FIE,GIP,VOL,Z,DZ)
IMPLICIT REAL*8(A-H,O-Z,$)
DIMENSION X(L),U(L),P(L),RO(L),G(L),E(L),DU(L),DP(L),DRO(L),
DG(L),DXSI(L),MIN(L),
US(L),PS(L),UIDOT(L),PIDOT(L)
,TENA(L),FIRO(L),FIM(L),FIE(L)
,GIP(L),VOL(L),Z(L),DZ(L)
,FIMZ(L),ZMDOT(L)
COMMON /TOT/AMTOT,ETOT,EKTOT,EPTOT,TENTOT
COMMON /STEP0/UL,PL,ROL,GL,UR,PR,ROR,GR,USTAR,PSTAR,
RSTARL,RSTARR,GSTARL,GSTARR,
CL,CR,CSTARL,CSTARR,SL,SR,WL,WR,UW(6)
,LAMDAL,LAMDAR,RATEL,RATER,TEMPL,TEMPR,TEMPSL,TEMPSR
,ZL,ZR,ZSTARL,ZSTARR,NFLUX,HELEML,HELEMR
REAL*8 LAMDAL,LAMDAR
LOGICAL HELEML,HELEMR
COMMON /AB/A(50)
EQUIVALENCE (LL,A(2)),(T,A(3)),(NCYC,A(12)),(DT,A(4))
EQUIVALENCE (UGAL,A(15))
COMMON/DIFFUS/U2,P2,RO2,ARW
COMMON/DETO/QDET,PCJDET,RCJDET,UCJDET,DCJDET,PODET,ROODET,
RATE,TEMPC
COMMON /GAM/GAMA,NG,MU2,G1,G2,G3,G4,G5,G6,G7,G8,G9,G10,G11
,G12,G13,G14,G15,G16,G17,G18,G19,G20,G21,G22,G23
,G24,G25,G26,G27,G28,G29,G30,G31,G32,G33,G34,G35
REAL*8 NG,MU2
COMMON /MONIT/CASEAV(4),NC14(4),NF16(6),
NMONU(4),NMONP(4),NMONRO(4),NMONZ(4)
DIMENSION CASAV1(4)
LOGICAL FULLPR
*****
FULLPR=.TRUE.
PRINT 1
FORMAT(1H1)
PRINT 2, T,DT,NCYC
FORMAT(1X,10X,'RESULTS AT T=',D11.5,5X,'DT=',D11.5,5X,'NCYC=',
I5//)
PRINT 3, AMTOT,ETOT,EKTOT,EPTOT,TENTOT
FORMAT(1X,'AMTOT=',D20.14,2X,'ETOT,EKTOT,EPTOT=',3D22.14/
1X,'TENTOT=',D21.14//)
FORMAT(1X,' I',
X U P
RO G Z
DU DP DRO
DG DZ')
FORMAT(1X,'
ZMDOT FIMZ AMDOT
AMDOTN TEMP ENTALP
AMACH ENTRO ')
FORMAT(1X)
IF (UGAL.NE.0.) PRINT 6, UGAL
FORMAT(/11X,'INITIAL VELOCITY CORRESPONDS TO UGAL=',D15.6/)
DO 10 I=1,L
IF (MOD(I,10).NE.1) GO TO 11

```

```

PRINT 5
PRINT 4
PRINT 44
PRINT 5
11 CONTINUE
PRINT 12,I,X(I),U(I),P(I),RO(I),G(I),Z(I),DU(I),DP(I),DRO(I),
1 DG(I),DZ(I)
12 FORMAT(1X,I3,6D12.5,5D11.4)
ENTRO=P(I)/RO(I)**GAMA
IF(.NOT.FULLPR) GO TO 131
IF(I.EQ.1) GO TO 131
IM=I-1
UL=U(IM)+0.5*DU(IM)
PL=P(IM)+0.5*DP(IM)
ROL=RO(IM)+0.5*DRO(IM)
GL=G(IM)+0.5*DG(IM)
CL=GL/ROL
ZL=Z(IM)+0.5*DZ(IM)
IF(ZL.LT.0.) ZL=0.
UR=U(I)-0.5*DU(I)
PR=P(I)-0.5*DP(I)
GR=G(I)-0.5*DG(I)
ROR=RO(I)-0.5*DRO(I)
CR=GR/ROR
ZR=Z(I)-0.5*DZ(I)
IF(ZR.LT.0.) ZR=0.
IF(PL.LE.0.) PL=1.D-8
IF(PR.LE.0.) PR=1.D-8
CALL RIEMAN(L,I,MIN)
XI=X(I)
RSTAR=RSTARL
IF(USTAR.LT.0.) RSTAR=RSTARR
ZSTAR=ZL
IF(USTAR.LT.0.) ZSTAR=ZR
AMACH=USTAR/DSQRT(GAMA*PSTAR/RSTAR)
AMDOT=RSTAR*USTAR*CROSS(XI)
IF(I.NE.2) GO TO 132
AMDOT0=AMDOT
IF(DABS(AMDOT0).LT.1.D-12) AMDOT0=1.D0
132 CONTINUE
AMDOTN=AMDOT/AMDOT0
ENTALP=(GAMA/(GAMA-1.D0))*PSTAR/RSTAR+0.5D0*USTAR**2+QDET*ZSTAR
ARW=1.D0
TEMP=PSTAR/(RSTAR*ARW)
PRINT 13,US(I),PS(I),
1 ZMDOT(I),FIMZ(I),AMDOT,AMDOTN,TEMP,ENTALP,AMACH,ENTRO
13 FORMAT(4X,12X,5D12.5,6D11.4)
131 CONTINUE
10 CONTINUE
C JOB STATISTICS
DO 40 I=1,4
CASAV1(I)=0.
IF (NC14(I).NE.0) CASAV1(I)=CASEAV(I)/DFLOAT(NC14(I))
40 CONTINUE
PRINT 30
30 FORMAT(///1X,10('*'),3X,'JOB STATISTICS',3X,10('*')//)
PRINT 31,(NC14(I),I=1,4)
31 FORMAT(1X,'NO. OF VARIOUS CASES IN RIEMAN SOLVER NC14(NCASE)=' ,
1 4I10)
PRINT 301, (CASAV1(I),I=1,4)
301 FORMAT(/1X,'AVERAGE NUMBER OF ITERATIONS IN RIEMAN SOLVER',
1 1X,' CASAV1(NCASE)=' ,4(F6.2,4X))
PRINT 32,(NF16(I),I=1,6)
32 FORMAT(/1X,'NO. OF VARIOUS FLUX CASES NF16(NFLUX)=' ,6I10)
ICATO=4
PRINT 33,(NMONU(I),I=1,ICATO),(NMONP(I),I=1,ICATO),
1 (NMONRO(I),I=1,ICATO),(NMONZ(I),I=1,ICATO)
33 FORMAT(/1X,'NO. OF MONOTONICITY INTERVENTIONS FOR EACH VAR.',
1 1X,'IN EACH CATEGORY.'/
1 1X,'NMONU (ICAT)=' ,4I10/
1 1X,'NMONP (ICAT)=' ,4I10/
1 1X,'NMONRO(ICAT)=' ,4I10/

```

1	1X, 'NMONZ (ICAT)=' ,4I10/)	CHA1030
	RETURN	CHA1031
	END	CHA1032
	SUBROUTINE SOF(ISTOP)	CHA1034
	IMPLICIT REAL*8(A-H,O-Z,\$)	CHA1035
	DIMENSION ISTOP(1)	CHA1036
	PRINT 1, ISTOP	CHA1037
	FORMAT(/1X,3H***,3X,20A4,3X,3H***//)	CHA1038
	PRINT 1	CHA1039
	XX=-1.D0	CHA1040
	YY=DSQRT(XX)	CHA1041
	STOP	CHA1042
	END	CHA1043
	SUBROUTINE RIEMAN(L,I,MIN)	CHA1310
	IMPLICIT REAL*8(A-H,O-Z,\$)	CHA1311
	DIMENSION MIN(L)	CHA1312
	COMMON /STEP0/UL,PL,ROL,GL,UR,PR,ROR,GR,USTAR,PSTAR,	CHA1313
1	RSTARL,RSTARR,GSTARL,GSTARR,	CHA1314
2	CL,CR,CSTARL,CSTARR,SL,SR,WL,WR,UW(6)	CHA1315
3	,LAMDAL,LAMDAR,RATEL,RATER,TEMPL,TEMPSR	CHA1316
4	,ZL,ZR,ZSTARL,ZSTARR,NFLUX,HELEML,HELEMR	CHA1317
	REAL*8 LAMDAL,LAMDAR	CHA1318
	LOGICAL HELEML,HELEMR	CHA1319
	COMMON /STEP1/DUIDT,DPIDT,DGIDTL,DGIDTR,DRIDTL,DRIDTR	CHA1320
2	,ASTARL,ASTARR,LAMDSL,LAMDSR,DSDAL,DSDAR,DZDAL,DZDAR	CHA1321
3	,RAT,SH	CHA1322
4	,BETA CL,BETACR,DSDASL,DSDASR,DZDASL,DZDASR	CHA1323
	REAL*8 LAMDSL,LAMDSR,DSDAL,DSDAR,DZDAL,DZDAR	CHA1324
	COMMON /DRAW/GODELX,GODELY,UMIN,UMAX,PMIN,PMAX,ROMIN,ROMAX	CHA1325
1	,XMIN,XMAX,SMIN,SMAX,IVERSA	CHA1326
	COMMON /GAM/GAMA,NG,MU2,G1,G2,G3,G4,G5,G6,G7,G8,G9,G10,G11	CHA1327
1	,G12,G13,G14,G15,G16,G17,G18,G19,G20,G21,G22,G23	CHA1328
2	,G24,G25,G26,G27,G28,G29,G30,G31,G32,G33,G34,G35	CHA1329
	REAL*8 NG,MU2	CHA1330
	COMMON /AB/A(50)	CHA1331
	COMMON /MONIT/CASEAV(4),NC14(4),NF16(6),	CHA1332
1	NMONU(4),NMONP(4),NMONRO(4),NMONZ(4)	CHA1333
	XX	CHA1334
	DATA NMAX/63/	CHA1335
	DATA EPS/1.D-8/	CHA1336
	DATA NTRY/0/	CHA1337
	XX	CHA1338
	UW(6)=1.D20	CHA1339
	WL=0.	CHA1340
	WR=0.	CHA1341
	ZETAL=PL*G8	CHA1342
	ZETAR=PR*G8	CHA1343
	CLG=CL/GAMA	CHA1344
	CRG=CR/GAMA	CHA1345
	ZSTARL=ZL	CHA1346
	ZSTARR=ZR	CHA1347
	IF (ZETAL.LT.ZETAR) GO TO 102	CHA1348
	LEFT PRESSURE IS HIGHER	CHA1349
01	CONTINUE	CHA1350
	EVERR=(PL-PR)/PR	CHA1351
	USR=UR+CRG*EVERR/DSQRT(1.D0+G6*EVERR)	CHA1352
	SRR=USR	CHA1353
	UEL=UL-G7*CL*(ZETAR-ZETAL)/ZETAL	CHA1354
	SLL=UEL	CHA1355
	NL=2	CHA1356
	NR=2	CHA1357
	IF (USR.GE.UL) NL=1	CHA1358
	IF (UEL.LE.UR) NR=1	CHA1359
	IF (DABS(EVERR).LT.EPS) GO TO 100	CHA1360
	IF (NL.EQ.2.AND.NR.EQ.1) GO TO 7001	CHA1361
	GO TO 100	CHA1362
	RIGHT PRESSURE IS HIGHER	CHA1363
02	CONTINUE	CHA1364
	EVERL=(PR-PL)/PL	CHA1365
	USL=UL-CLG*EVERL/DSQRT(1.D0+G6*EVERL)	CHA1366
	SLL=USL	CHA1367
	UER=UR+G7*CR*(ZETAL-ZETAR)/ZETAR	CHA1368

	SRR=UER	CHA1369
	NL=2	CHA1370
	NR=2	CHA1371
	IF (UER.GE.UL) NL=1	CHA1372
	IF (USL.LE.UR) NR=1	CHA1373
	IF (DABS(EVERL).LT.EPS) GO TO 100	CHA1374
	IF (NL.EQ.1.AND.NR.EQ.2) GO TO 7001	CHA1375
	GO TO 100	CHA1376
100	CONTINUE	CHA1377
	IF (NL.EQ.1.AND.NR.EQ.2) NCASE=1	CHA1378
	IF (NL.EQ.2.AND.NR.EQ.2) NCASE=2	CHA1379
	IF (NL.EQ.2.AND.NR.EQ.1) NCASE=3	CHA1380
	IF (NL.EQ.1.AND.NR.EQ.1) NCASE=4	CHA1381
	IF(DABS(PL-PR)+DABS(UL-UR).LT.EPS*(PMAX-UMIN)) NCASE=4	CHA1382
	UMIDA=EPS*DMAX1(CL,CR)	CHA1383
	DUDZL=-G7*CL/ZETAL	CHA1384
	DUDZR= G7*CR/ZETAR	CHA1385
	ZETA=(-(UR-UL)+ZETAR*DUDZR-ZETAL*DUDZL)/(DUDZR-DUDZL)	CHA1386
	IF (ZETA.LE.0.) GO TO 7002	CHA1387
	N=0	CHA1388
	GO TO (1,2,3,4), NCASE	CHA1389
C	THE CASE ES	CHA1390
1	ITYPE=NCASE	CHA1391
	HELEML=.FALSE.	CHA1392
	HELEMR=.TRUE.	CHA1393
11	N=N+1	CHA1394
	IF (N.GT.NMAX) GO TO 7003	CHA1395
	ZETAF=ZETA	CHA1396
	UEL=UL-G7*CL*(ZETAF-ZETAL)/ZETAL	CHA1397
	PPR=(ZETAF/ZETAR)**NG	CHA1398
	EVERR=PPR-1.DO	CHA1399
	SQRR=DSQRT(1.DO+G6*EVERR)	CHA1400
	USR=UR+CRG*EVERR/SQRR	CHA1401
	DU=UEL-USR	CHA1402
	IF (DABS(DU).LE.UMIDA) GO TO 10	CHA1403
	DUDZR=NG*CRG*(PPR/ZETAF)*(1.DO+G9*EVERR)/SQRR**3	CHA1404
	ZETA=ZETAF+DU/(DUDZR-DUDZL)	CHA1405
	GO TO 11	CHA1406
10	CONTINUE	CHA1407
	USTAR=(UEL+USR)/2.DO	CHA1408
	IF(DABS(USTAR).LT.EPS*UMAX) USTAR=0.	CHA1409
	PSTAR=PPR*PR	CHA1410
	CSTARL=CL+(UL-USTAR)/G7	CHA1411
	RSTARL=GAMA*PSTAR/CSTARL**2	CHA1412
	GSTARL=CSTARL*RSTARL	CHA1413
C	EQU. NO. 69.01 OF THE BOOK BY COURANT-FRIEDRICHS.	CHA1414
	WWR=G11*(USTAR-UR)*ROR	CHA1415
	WR=WWR+DSQRT(GR**2+WWR**2)	CHA1416
	RSTARR=ROR*WR/(WR-ROR*(USTAR-UR))	CHA1417
	GSTARR=DSQRT(GAMA*PSTAR*RSTARR)	CHA1418
	CSTARR=GSTARR/RSTARR	CHA1419
	WRE=WR/ROR+UR	CHA1420
	UW(1)=UL-CL	CHA1421
	UW(2)=USTAR-CSTARL	CHA1422
	UW(3)=USTAR	CHA1423
	UW(4)=WRE	CHA1424
	UW(5)=WRE	CHA1425
	GO TO 5	CHA1426
C	THE CASE SS	CHA1427
2	ITYPE=NCASE	CHA1428
	HELEML=.TRUE.	CHA1429
	HELEMR=.TRUE.	CHA1430
21	N=N+1	CHA1431
	IF (N.GT.NMAX) GO TO 7003	CHA1432
	ZETAF=ZETA	CHA1433
	PF=ZETAF**NG	CHA1434
	PPL=PF/PL	CHA1435
	PPR=PF/PR	CHA1436
	EVERL=PPL-1.DO	CHA1437
	EVERR=PPR-1.DO	CHA1438
	SQRL=DSQRT(1.DO+G6*EVERL)	CHA1439
	SQRR=DSQRT(1.DO+G6*EVERR)	CHA1440

```

USL=UL-CLG*EVERL/SQRL
USR=UR+CRG*EVERR/SQRR
DU=USL-USR
IF (DABS(DU).LE.UMIDA) GO TO 20
DUDZL=-NG*CLG*(PPL/ZETAF)*(1.D0+G9*EVERL)/SQRL**3
DUDZR= NG*CRG*(PPR/ZETAF)*(1.D0+G9*EVERR)/SQRR**3
ZETA=ZETAF+DU/(DUDZR-DUDZL)
GO TO 21
CONTINUE
0 USTAR=(USL+USR)/2.D0
IF(DABS(USTAR).LT.EPS*UMAX) USTAR=0.
PSTAR=(PPL*PL+PPR*PR)/2.D0
WWR=G11*(USTAR-UR)*ROR
WR=WWR+DSQRT(GR**2+WWR**2)
WWL=-G11*(USTAR-UL)*ROL
WL=WWL+DSQRT(GL**2+WWL**2)
RSTARL=ROL*WL/(WL+ROL*(USTAR-UL))
RSTARR=ROR*WR/(WR-ROR*(USTAR-UR))
GSTARL=DSQRT(GAMA*PSTAR*RSTARL)
GSTARR=DSQRT(GAMA*PSTAR*RSTARR)
CSTARL=GSTARL/RSTARL
CSTARR=GSTARR/RSTARR
WLE=-WL/ROL+UL
WRE=WR/ROR+UR
UW(1)=WLE
UW(2)=WLE
UW(3)=USTAR
UW(4)=WRE
UW(5)=WRE
GO TO 5
THE CASE SE
ITYPE=NCASE
HELEML=.TRUE.
HELEMR=.FALSE.
1 N=N+1
IF (N.GT.NMAX) GO TO 7003
ZETAF=ZETA
UER=UR+G7*CR*(ZETAF-ZETAR)/ZETAR
PPL=(ZETAF/ZETAL)**NG
EVERL=PPL-1.D0
SQRL=DSQRT(1.D0+G6*EVERL)
USL=UL-CLG*EVERL/SQRL
DU=USL-UER
IF (DABS(DU).LE.UMIDA) GO TO 30
DUDZL=-NG*CLG*(PPL/ZETAF)*(1.D0+G9*EVERL)/SQRL**3
ZETA=ZETAF+DU/(DUDZR-DUDZL)
GO TO 31
CONTINUE
0 USTAR=(USL+UER)/2.D0
IF(DABS(USTAR).LT.EPS*UMAX) USTAR=0.
PSTAR=PPL*PL
CSTARR=CR-(UR-USTAR)/G7
RSTARR=GAMA*PSTAR/CSTARR**2
GSTARR=CSTARR*RSTARR
WWL=-G11*(USTAR-UL)*ROL
WL=WWL+DSQRT(GL**2+WWL**2)
WLE=-WL/ROL+UL
RSTARL=ROL*WL/(WL+ROL*(USTAR-UL))
GSTARL=DSQRT(GAMA*PSTAR*RSTARL)
CSTARL=GSTARL/RSTARL
UW(1)=WLE
UW(2)=WLE
UW(3)=USTAR
UW(4)=USTAR+CSTARR
UW(5)=UR+CR
GO TO 5
THE CASE EE
ITYPE=NCASE
HELEML=.FALSE.
HELEMR=.FALSE.
PSTAR=ZETA**NG
USTAR=UL-G7*CL*(ZETA-ZETAL)/ZETAL

```

CHA1441
CHA1442
CHA1443
CHA1444
CHA1445
CHA1446
CHA1447
CHA1448
CHA1449
CHA1450
CHA1451
CHA1452
CHA1453
CHA1454
CHA1455
CHA1456
CHA1457
CHA1458
CHA1459
CHA1460
CHA1461
CHA1462
CHA1463
CHA1464
CHA1465
CHA1466
CHA1467
CHA1468
CHA1469
CHA1470
CHA1471
CHA1472
CHA1473
CHA1474
CHA1475
CHA1476
CHA1477
CHA1478
CHA1479
CHA1480
CHA1481
CHA1482
CHA1483
CHA1484
CHA1485
CHA1486
CHA1487
CHA1488
CHA1489
CHA1490
CHA1491
CHA1492
CHA1493
CHA1494
CHA1495
CHA1496
CHA1497
CHA1498
CHA1499
CHA1500
CHA1501
CHA1502
CHA1503
CHA1504
CHA1505
CHA1506
CHA1507
CHA1508
CHA1509
CHA1510
CHA1511
CHA1512

```

IF(DABS(USTAR).LT.EPS*UMAX) USTAR=0.
CSTARL=CL+(UL-USTAR)/G7
CSTARR=CR-(UR-USTAR)/G7
RSTARL=GAMA*PSTAR/CSTARL**2
RSTARR=GAMA*PSTAR/CSTARR**2
GSTARL=RSTARL*CSTARL
GSTARR=RSTARR*CSTARR
UW(1)=UL-CL
UW(2)=USTAR-CSTARL
UW(3)=USTAR
UW(4)=USTAR+CSTARR
UW(5)=UR+CR
N=1
GO TO 5
5 CONTINUE
DO 6 K=1,6
NFLUX=K
IF (UW(K).GE.0.) GO TO 61
6 CONTINUE
NFLUX=6
61 CONTINUE
NC14(NCASE)=NC14(NCASE)+1
CASEAV(NCASE)=CASEAV(NCASE)+DFLOAT(N)
NF16(NFLUX)=NF16(NFLUX)+1
IF(NTRY.GE.2)GO TO 666
IF(I.NE.2.AND.I.NE.L) GO TO 666
PRINT 667,I,NFLUX,NCASE,PL,UL,ROL,PR,UR,ROR,USTAR,PSTAR,RSTARL,
1 RSTARR,(KK,UW(KK),KK=1,6)
667 FORMAT(/1X,'I,NFLUX,NCASE=',3I5/1X,'PL,UL,ROL,PR,UR,ROR=',6D12.4/
1 1X,'USTAR,PSTAR,RSTARL,RSTARR=',4D13.4/
2 1X,'KK,UW(KK)=' ,6(I4,2X,D13.4)/)
NTRY=NTRY+1
666 CONTINUE
RETURN
7001 CONTINUE
PRINT 7101, PL,UL,PR,UR,ZETAL,ZETAR,SLL,SRR,NL,NR,I
7101 FORMAT(//1X,'FROM RIEMAN. AN IMPOSSIBLE CASE OF EXPANSION/SHOCK'
1 //1X,'PL,UL,PR,UR=' ,4D25.14//
2 1X,'ZETAL,ZETAR,SLL,SRR=' ,4D25.14//
3 1X,'NL,NR,I=' ,3I10//)
CALL SOF('7001')
7002 CONTINUE
PRINT 7102, ZETA,DUDZL,DUDZR,ZETAL,ZETAR,PL,UL,PR,UR,N,NCASE,I
7102 FORMAT(//1X,'FROM RIEMAN. NEGATIVE PRESSURE AT THE INTERSECTION',
1 1X,'OF L AND R EXPANSION BRANCHES'//
2 1X,'IT MEANS THAT A CAVITATION TENDS TO FORM. THIS',
3 1X,'POSSIBILITY IS EXCLUDED IN PRESENT VERSION'//
4 1X,'ZETA,DUDZL,DUDZR,ZETAL,ZETAR,PL,UL,PR,UR=' ,9D10.3//
5 1X,'N,NCASE,I=' ,3I10//)
CALL SOF('7002')
7003 CONTINUE
PRINT 7103, I,N,NCASE,DU,UMIDA,EPS,PL,UL,PR,UR,
1 ZETA,ZETAF,ZETAL,ZETAR,DUDZL,DUDZR
7103 FORMAT(//1X,'FROM RIEMAN. NUMBER OF ITERATIONS EXCEEDED.'//
1 1X,'I,N,NCASE,DU,UMIDA,EPS=' ,3I6,3D18.6//
2 1X,'PL,UL,PR,UR,ZETA,ZETAF=' ,6D18.10//
3 1X,'ZETAL,ZETAR,DUDZL,DUDZR=' ,4D18.10//)
CALL SOF('7003')
RETURN
END
C$OPTIONS LIST
SUBROUTINE MAGA(L,I,MIN)
IMPLICIT REAL*8(A-H,O-Z,$)
DIMENSION MIN(L)
COMMON /GAM/GAMA,NG,MU2,G1,G2,G3,G4,G5,G6,G7,G8,G9,G10,G11
1 ,G12,G13,G14,G15,G16,G17,G18,G19,G20,G21,G22,G23
2 ,G24,G25,G26,G27,G28,G29,G30,G31,G32,G33,G34,G35
REAL*8 NG,MU2
COMMON/DETO/QDET,PCJDET,RCJDET,UCJDET,DCJDET,PODET,ROODET,
1 RATE,TEMPC
COMMON /STEP0/UL,PL,ROL,GL,UR,PR,ROR,GR,USTAR,PSTAR,
1 RSTARL,RSTARR,GSTARL,GSTARR,

```

MAGA

```

2          CL,CR,CSTARL,CSTARR,SL,SR,WL,WR,UW(6)          CHA1588
3          ,LAMDAL,LAMDAR,RATEL,RATER,TEMPL,TEMPL,TEMPSL,TEMPSR CHA1589
4          ,ZL,ZR,ZSTARL,ZSTARR,NFLUX,HELEML,HELEMR      CHA1590
REAL*8 LAMDAL,LAMDAR          CHA1591
LOGICAL HELEML,HELEMR      CHA1592
COMMON /STEP1/DUIDT,DPIDT,DGIDTL,DGIDTR,DRIDTL,DRIDTR    CHA1593
2          ,ASTARL,ASTARR,LAMDSL,LAMDSR,DSDAL,DSDAR,DZDAL,DZDAR CHA1594
3          ,RAT,SH          CHA1595
4          ,BETACL,BETACR,DSDASL,DSDASR,DZDASL,DZDASR    CHA1596
REAL*8 LAMDSL,LAMDSR,DSDAL,DSDAR,DZDAL,DZDAR          CHA1597
COMMON /GRADS/DUDXIL,DPDXIL,DGDIXIL,DRDXIL,DZDXIL,DSDXIL, CHA1598
1          DUDXIR,DPDXIR,DGDIXIR,DRDXIR,DZDXIR,DSDXIR    CHA1599
COMMON /AB/A(50)          CHA1600
REAL*8 LU,LP,LRO,LLAMDA    CHA1601
DATA EPS/1.D-6/          CHA1602
XXXXXXXXXXXXXXXXXXXXXXXXXXXXXXXXXXXXXXXXXXXXXXXXXXXXXXXXXXXXXXXXXXXXXXXXXXXX CHA1603
WE HERE SOLVE FOR THE TIME-DERIVATIVES ALONG THE CONTACT SURFACE, CHA1604
NAMELY DUIDT,DPIDT. FROM THESE WE ALSO OBTAIN THE OTHER CHA1605
TIME-DERIVATIVES (SEE COMMON /STEP1/). CHA1606
WE COMPUTE THE COEFFICIENTS FOR TWO EQUATIONS FOR DUIDT,DPIDT. THESE CHA1607
ARE          AAL*DUIDT+BBL*DPIDT=DDL CHA1608
          AAR*DUIDT+BBR*DPIDT=DDR CHA1609
XXXXXXXXXXXXXXXXXXXXXXXXXXXXXXXXXXXXXXXXXXXXXXXXXXXXXXXXXXXXXXXXXXXXXXXXXXXX CHA1610
IF(SH.LE.EPS)RAT=0. CHA1611
LEFT SIDE OF CONTACT CHA1612
IF (.NOT.HELEML) GO TO 12 CHA1613
11 CONTINUE CHA1614
LEFT SHOCK CHA1615
DP=PSTAR-PL CHA1616
DU=USTAR-UL CHA1617
Z2=0.5D0/(PSTAR+MU2*PL) CHA1618
LU=DU*(0.5D0*ROL+MU2*Z2*GL**2)-GL**2/WL-WL CHA1619
LRO=-0.5D0*DP/ROL CHA1620
LP=-2.D0-MU2*Z2*DP CHA1621
AAL=2.D0-Z2*DP CHA1622
BBL=Z2*DU+WL/GSTARL**2+1.D0/WL CHA1623
DDL=LU*DUDXIL+LRO*DRDXIL+LP*DPDXIL CHA1624
DDL=DDL-WL*USTAR*RAT/RSTARL CHA1625
1 +UL*RAT*(-GAMA*PL/WL+DU*(GAMA*PL*MU2*Z2+0.5D0)) CHA1626
GO TO 10 CHA1627
12 CONTINUE CHA1628
LEFT RAREFACTION CHA1629
A1=DUDXIL+DPDXIL/GL CHA1630
BETA=GSTARL/GL CHA1631
SQB=DSQRT(BETA) CHA1632
ASTARL=A1-(CL/(G15*SL))*DSDXIL*(BETA**G5-1.D0) CHA1633
AAL=1.D0 CHA1634
BBL=1.D0/GSTARL CHA1635
DDL=-GSTARL*ASTARL/SQB CHA1636
DSDAL=DSDXIL CHA1637
DZDAL=DZDXIL CHA1638
DSDASL=DSDXIL*SQB CHA1639
DZDASL=DZDXIL*SQB CHA1640
GEOM=RAT*((GAMA-1.D0)*UL+2.D0*CL)* CHA1641
1 (BETA**G13-1.D0)/(ROL*(GAMA-3.D0)) CHA1642
1 -4.D0*RAT*CL*(BETA**G14-1.D0)/(ROL*(3.D0*GAMA-5.D0)) CHA1643
ASTARL=ASTARL-GEOM CHA1644
EVER1= GSTARL*GEOM/SQB CHA1645
EVER2=-RAT*USTAR*CSTARL CHA1646
DDL=DDL+EVER1+EVER2 CHA1647
GO TO 10 CHA1648
10 CONTINUE CHA1649
RIGHT SIDE OF CONTACT CHA1650
IF (.NOT.HELEMR) GO TO 22 CHA1651
21 CONTINUE CHA1652
RIGHT SHOCK CHA1653
DP=PSTAR-PR CHA1654
DU=USTAR-UR CHA1655

```

```

Z2=0.5D0/(PSTAR+MU2*PR)
LU=DU*(0.5D0*ROR+MU2*Z2*GR**2)+GR**2/WR+WR
LRO=-0.5D0*DP/ROR
LP=-2.D0-MU2*Z2*DP
AAR=2.D0-Z2*DP
BBR=Z2*DU-WR/GSTARR**2-1.D0/WR
DDR=LU*DUDXIR+LRO*DRDXIR+LP*DPDXIR
DDR=DDR+WR*USTAR*RAT/RSTARR
1   +UR*RAT*(GAMA*PR/WR+DU*(GAMA*PR*MU2*Z2+0.5D0))
GO TO 20
22  CONTINUE
C   RIGHT RAREFACTION
A1=DUDXIR-DPDXIR/GR
BETA=GSTARR/GR
SQB=DSQRT(BETA)
ASTARR=A1+(CR/(G15*SR))*DSDXIR*(BETA**G5-1.D0)
AAR=1.D0
BBR=-1.D0/GSTARR
DDR=GSTARR*ASTARR/SQB
DSDAR=DSDXIR
DZDAR=DZDXIR
DSDASR=DSDXIR*SQB
DZDASR=DZDXIR*SQB
GEOM=RAT*(-(GAMA-1.D0)*UR+2.D0*CR)*(BETA**G13-1.D0)
1   /(ROR*(GAMA-3.D0))
2   -4.D0*RAT*CR*(BETA**G14-1.D0)/(ROR*(3.D0*GAMA-5.D0))
ASTARR=ASTARR+GEOM
EVER1=GSTARR*GEOM/SQB
EVER2=RAT*USTAR*CSTARR
DDR=DDR+EVER1+EVER2
GO TO 20
20  CONTINUE
DET=AAL*BBR-AAR*BBL
DUIDT=(DDL*BBR-DDR*BBL)/DET
DPIDT=- (DDL*AAR-DDR*AAL)/DET
DRIDTL=DPIDT/CSTARL**2
DRIDTR=DPIDT/CSTARR**2
RETURN
END
SUBROUTINE FLUXE(L,I,MIN)
IMPLICIT REAL*8(A-H,O-Z,$)
DIMENSION MIN(L)
COMMON /AB/A(50)
EQUIVALENCE (DT,A(4)),(NCYC,A(12))
COMMON /GAM/GAMA,NG,MU2,G1,G2,G3,G4,G5,G6,G7,G8,G9,G10,G11
1   ,G12,G13,G14,G15,G16,G17,G18,G19,G20,G21,G22,G23
2   ,G24,G25,G26,G27,G28,G29,G30,G31,G32,G33,G34,G35
REAL*8 NG,MU2
COMMON /GRADS/DUDXIL,DPDXIL,DGDXIL,DRDXIL,DZDXIL,DSDXIL,
1   DUDXIR,DPDXIR,DGDXIR,DRDXIR,DZDXIR,DSDXIR
COMMON /STEP0/UL,PL,ROL,GL,UR,PR,ROR,GR,USTAR,PSTAR,
1   RSTARL,RSTARR,GSTARL,GSTARR,
2   CL,CR,CSTARL,CSTARR,SL,SR,WL,WR,UW(6)
3   ,LAMDAL,LAMDAR,RATEL,RATER,TEMPL,TEMPR,TEMPSL,TEMPSR
4   ,ZL,ZR,ZSTARL,ZSTARR,NFLUX,HELEML,HELEMR
REAL*8 LAMDAL,LAMDAR
LOGICAL HELEML,HELEMR
COMMON /STEP1/DUIDT,DPIDT,DGIDTL,DGIDTR,DRIDTL,DRIDTR
2   ,ASTARL,ASTARR,LAMDSL,LAMDSR,DSDAL,DSDAR,DZDAL,DZDAR
3   ,RAT,SH
4   ,BETACL,BETACR,DSDASL,DSDASR,DZDASL,DZDASR
REAL*8 LAMDSL,LAMDSR,DSDAL,DSDAR,DZDAL,DZDAR
COMMON/DETO/QDET,PCJDET,RCJDET,UCJDET,DCJDET,PODET,ROODET,
1   RATE,TEMPC
COMMON /FI/FIH1,FIH2,FIH3,UXN,PXN,GXN,ROXN,ZXN
1   ,GIH
2   ,FIH4,ZMDOTL,ZMDOTR
REAL*8 LAMDAO
C*****
C RO,U,P,Z AND THEIR (XI,T) DERIVATIVES AT EULERIAN POINT X=X(I).
C*****
DT2=DT/2.D0

```

CHA1660
CHA1661
CHA1662
CHA1663
CHA1664
CHA1665
CHA1666
CHA1667
CHA1668
CHA1669
CHA1670
CHA1671
CHA1672
CHA1673
CHA1674
CHA1675
CHA1676
CHA1677
CHA1678
CHA1679
CHA1680
CHA1681
CHA1682
CHA1683
CHA1684
CHA1685
CHA1686
CHA1687
CHA1688
CHA1689
CHA1690
CHA1691
CHA1692
CHA1693
CHA1694
CHA1695
CHA1696
CHA1697
CHA1698
FLUXE
CHA1699
CHA1700
CHA1701
CHA1702
CHA1703
CHA1704
CHA1705
CHA1706
CHA1707
CHA1708
CHA1709
CHA1710
CHA1711
CHA1712
CHA1713
CHA1714
CHA1715
CHA1716
CHA1717
CHA1718
CHA1719
CHA1720
CHA1721
CHA1722
CHA1723
CHA1724
CHA1725
CHA1726
CHA1727
CHA1728
CHA1729
CHA1730
CHA1731

GO TO (1,2,3,4,5,6),NFLUX
CONTINUE

CHA1732
CHA1733
CHA1734
CHA1735
CHA1736
CHA1737
CHA1738
CHA1739
CHA1740
CHA1741
CHA1742
CHA1743
CHA1744
CHA1745
CHA1746
CHA1747
CHA1748
CHA1749
CHA1750
CHA1751
CHA1752
CHA1753
CHA1754
CHA1755
CHA1756
CHA1757
CHA1758
CHA1759
CHA1760
CHA1761
CHA1762
CHA1763
CHA1764
CHA1765
CHA1766
CHA1767
CHA1768
CHA1769
CHA1770
CHA1771
CHA1772
CHA1773
CHA1774
CHA1775
CHA1776
CHA1777
CHA1778
CHA1779
CHA1780
CHA1781
CHA1782
CHA1783
CHA1784
CHA1785
CHA1786
CHA1787
CHA1788
CHA1789
CHA1790
CHA1791
CHA1792
CHA1793
CHA1794
CHA1795
CHA1796
CHA1797
CHA1798
CHA1799
CHA1800
CHA1801
CHA1802
CHA1803

NFLUX=1. LINE X=0 IS TO THE LEFT OF LEFT WAVE.

UX=UL
PX=PL
ROX=ROL
ZX=ZL
GX=GL
DUDXIX=DUDXIL
DPDXIX=DPDXIL
DRDXIX=DRDXIL
DZDXIX=DZDXIL
DUDTX=-DPDXIL
DRODTX=-ROL**2*DUDXIL
DPDTX=-GL**2*DUDXIL
DRODTX=DRODTX-RAT*ROL*UL
DPDTX=DPDTX*CL**2
DZDTX=0.
GO TO 9
CONTINUE

NFLUX=6. LINE X=0 IS TO THE RIGHT OF RIGHT WAVE.

UX=UR
PX=PR
ROX=ROR
ZX=ZR
GX=GR
DUDXIX=DUDXIR
DPDXIX=DPDXIR
DRDXIX=DRDXIR
DZDXIX=DZDXIR
DUDTX=-DPDXIR
DPDTX=-GR**2*DUDXIR
DRODTX=-ROR**2*DUDXIR
DRODTX=DRODTX-RAT*ROR*UR
DPDTX=DPDTX*CR**2
DZDTX=0.
GO TO 9
CONTINUE

NFLUX=2. SONIC CASE (LEFT).

BETA0=(MU2*(UL/CL+G7))**(.1.D0/MU2)
SQB0=DSQRT(BETA0)
A1=DUDXIL+DPDXIL/GL
A0=A1-(CL/(G15*SL))*DSDXIL*(BETA0**G5-1.D0)
EVER1=-((GAMA-1.D0)*UL+2.D0*CL)*(BETA0**G13-1.D0)/(GAMA-3.D0)
EVER2=4.D0*CL*(BETA0**G14-1.D0)/(3.D0*GAMA-5.D0)
EVER=(EVER1+EVER2)*RAT/ROL
A0=(A0+EVER)
DPDAX=GL*BETA0*A0
C0=MU2*(UL+G7*CL)
IF(C0.LT.0.) CALL SOF('FLUXE 2. C0 NEGATIVE.')

UX=C0
ROX=GL*BETA0/C0
ZX=ZL
PX=ROX*C0**2/GAMA
GX=ROX*C0
DPDAX=DPDAX+RAT*UX*C0*SQB0
DUDBX=-CL*BETA0**(-1.D0/G4)/G4
DPDBX=PL*BETA0**MU2/G6
DRODBX=ROL*BETA0**(-MU2)/G4
DSDAX=SQB0*DSDAL
DZDAX=SQB0*DZDAL
DRODAX=DPDAX/C0**2-(ROX/(GAMA*SL))*DSDAX
DUDAX=A0
DGDAX=0.5D0*GAMA*(PX*DRODAX+ROX*DPDAX)/GX
GO TO 9
CONTINUE

```

C
C   NFLUX=5.    SONIC CASE (RIGHT).
C
      BETA0=(MU2*(-UR/CR+G7))**(1.D0/MU2)
      SQB0=DSQRT(BETA0)
      A1=DUDXIR-DPDXIR/GR
      A0=A1+(CR/(G15*SR))*DSDXIR*(BETA0**G5-1.D0)
      EVER1=(-(GAMA-1.D0)*UR+2.D0*CR)*(BETA0**G13-1.D0)/(GAMA-3.D0)
      EVER2=-4.D0*CR*(BETA0**G14-1.D0)/(3.D0*GAMA-5.D0)
      EVER=(EVER1+EVER2)*RAT/ROR
      A0=(A0+EVER)
      DPDA=-GR*BETA0*A0
      C0=MU2*(-UR+G7*CR)
      IF(C0.LT.0.) CALL SOF('FLUXE 5.  C0 NEGATIVE.')
      UX=-C0
      ROX=GR*BETA0/C0
      ZX=ZR
      PX=ROX*C0**2/GAMA
      GX=ROX*C0
      DPDA=DPDA-RAT*UX*C0*DSQRT(BETA0)
      DUDBX=CR*BETA0**(-1.D0/G4)/G4
      DPDBX=PR*BETA0**MU2/G6
      DRODBX=ROR*BETA0**(-MU2)/G4
      DSDAX=SQB0*DSDAR
      DZDAX=SQB0*DZDAR
      DRODAX=DPDA/C0**2-(ROX/(GAMA*SR))*DSDAX
      DUDAX=A0
      DGDA=0.5D0*GAMA*(PX*DRODAX+ROX*DPDA)/GX
      GO TO 9
3    CONTINUE
C
C   NFLUX=3.    LINE X=0 IS BETWEEN THE LEFT WAVE AND THE CONTACT.
C
      UX=USTAR
      PX=PSTAR
      ROX=RSTARL
      ZX=ZL
      GX=GSTARL
      DUDXIX=-DPIDT/GSTARL**2
      DPDXIX=-DUIDT
      DUDXIX=DUDXIX-RAT*USTAR/RSTARL
      DZDXIX=DZDXIL
      DZDTX=0.
      IF(.NOT.HELEML) GO TO 32
31    CONTINUE
C   LEFT SHOCK.
      DRDXIX=(RSTARL/WL)**2*(3.D0*DUIDT
1         +DPIDT*(1.D0+3.D0*(WL/GSTARL)**2)/WL
2         +DUDXIL*WL*((GL/WL)**2+3.D0)+3.D0*DPDXIL
3         +DRDXIL*(WL/ROL)**2)
      EVER1=UL*RSTARL**2*RAT*((GL/WL)**2+1.D0)/(ROL*WL)
      EVER2=2.D0*RSTARL*USTAR*RAT/WL
      DRDXIX=DRDXIX+EVER1+EVER2
      DRODTX=-DUDXIX*ROX**2
      GO TO 33
32    CONTINUE
      BETA=GSTARL/GL
      SQB=DSQRT(BETA)
      DPDA=ASTARL*GSTARL
      DPDA=GSTARL*(ASTARL+RAT*USTAR*CSTARL/(GL*SQB))
      G41=1.D0/G4+0.5D0
      DRODA=(DRDXIL-DPDXIL/(CL*CL))*BETA**G41+DPDA/(CSTARL**2)
      DRDXIX=DRODA/SQB+DPIDT/(GSTARL*CSTARL**2)
      DRODA=DPDA/CSTARL**2-(RSTARL/(GAMA*SL))*DSDASL
      DRODTX=-DUDXIX*ROX**2
      DRDXIX=DRODA/SQB+DRODTX/GSTARL
33    CONTINUE
      DUDTX=DUIDT
      DPDTX=DPIDT
      GO TO 9
4    CONTINUE
C

```

CHA1804
CHA1805
CHA1806
CHA1807
CHA1808
CHA1809
CHA1810
CHA1811
CHA1812
CHA1813
CHA1814
CHA1815
CHA1816
CHA1817
CHA1818
CHA1819
CHA1820
CHA1821
CHA1822
CHA1823
CHA1824
CHA1825
CHA1826
CHA1827
CHA1828
CHA1829
CHA1830
CHA1831
CHA1832
CHA1833
CHA1834
CHA1835
CHA1836
CHA1837
CHA1838
CHA1839
CHA1840
CHA1841
CHA1842
CHA1843
CHA1844
CHA1845
CHA1846
CHA1847
CHA1848
CHA1849
CHA1850
CHA1851
CHA1852
CHA1853
CHA1854
CHA1855
CHA1856
CHA1857
CHA1858
CHA1859
CHA1860
CHA1861
CHA1862
CHA1863
CHA1864
CHA1865
CHA1866
CHA1867
CHA1868
CHA1869
CHA1870
CHA1871
CHA1872
CHA1873
CHA1874
CHA1875

```

NFLUX=4.   LINE X=0 IS BETWEEN THE CONTACT AND THE RIGHT WAVE.
DPDXIX=-DUIDT
UX=USTAR
PX=PSTAR
ROX=RSTARR
ZX=ZR
GX=GSTARR
DUDXIX=-DPIDT/GSTARR**2
DUDXIX=DUDXIX-RAT*USTAR/RSTARR
DPDXIX=-DUIDT
DZDXIX=DZDXIL
DZDTX=0.
IF (.NOT.HELEMR) GO TO 42
41 CONTINUE
RIGHT SHOCK
DRDXIX=(RSTARR/WR)**2*(3.*DUIDT
1 -DPIDT*(1.D0+3.D0*(WR/GSTARR)**2)/WR
2 -DUDXIR*WR*((GR/WR)**2+3.D0)+3.D0*DPDXIR
3 +DRDXIR*(WR/ROR)**2)
EVER1=UR*RSTARR**2*RAT*((GR/WR)**2+1.D0)/(ROR*WR)
EVER2=2.D0*RSTARR*USTAR*RAT/WR
DRDXIX=DRDXIX-EVER1-EVER2
DRODTX=-DUDXIX*ROX**2
GO TO 43
42 CONTINUE
RIGHT RAREFACTION
BETA=GSTARR/GR
SQB=DSQRT(BETA)
DPDA=-ASTARR*GSTARR
DPDA=-GSTARR*(ASTARR+RAT*USTAR*CSTARR/(GR* SQB))
G41=1.D0/G4+0.5D0
DRODA=(DRDXIR-DPDXIR/(CR*CR)) *BETA**G41+DPDA/(CSTARR**2)
DRDXIX= DRODA/SQB-DPIDT/(GSTARR*CSTARR**2)
DRODA=DPDA/CSTARR**2-(RSTARR/(GAMA*SR))*DSDASR
DRODTX=-DUDXIX*ROX**2
DRDXIX=DRODA/SQB-DRODTX/GSTARR
43 CONTINUE
DUDTX=DUIDT
DPDTX=DPIDT
GO TO 9
9 CONTINUE
*****
FLUXES CENTERED AT TIME T(N+1/2) AT EULERIAN POINT X=X(I).
*****
FI1=ROX*UX
FI2=ROX*UX**2+PX
FI2=FI2-PX
FI3=UX*(G12*PX+0.5D0*ROX*UX**2)
FI4=ZX*ROX*UX
FI3=FI3+QDET*FI4
ROU00=ROX*UX
GO TO(10,20,30,40,50,60), NFLUX
10 CONTINUE
60 CONTINUE
DFDXI1=DRDXIX*UX+ROX*DUDXIX
DFDXI2=DRDXIX*UX**2+2.D0*ROX*UX*DUDXIX+DPDXIX
DFDXI2=DFDXI2-DPDXIX
DFDXI3=DUDXIX*(G12*PX+0.5D0*ROX*UX**2)
1 +UX*(G12*DPDXIX+0.5D0*DRDXIX*UX**2+ROX*UX*DUDXIX)
DFDXI4=ZX*DFDXI1+ROX*UX*DZDXIX
DFDXI3=DFDXI3+QDET*DFDXI4
DFIDT1=DRODTX*UX+ROX*DUDTX
DFIDT2=DRODTX*UX**2+2.D0*ROX*UX*DUDTX+DPDTX
DFIDT2=DFIDT2-DPDTX
DFIDT3=DUDTX*(G12*PX+0.5D0*ROX*UX**2)
1 +UX*(G12*DPDTX+0.5D0*DRODTX*UX**2+ROX*UX*DUDTX)
DFIDT4=ZX*DFIDT1+ROX*ZX*DZDTX
DFIDT3=DFIDT3+QDET*DFIDT4
FIDOT1=-ROU00*DFDXI1+DFIDT1
FIDOT2=-ROU00*DFDXI2+DFIDT2
FIDOT3=-ROU00*DFDXI3+DFIDT3

```

CHA1876
CHA1877
CHA1878
CHA1879
CHA1880
CHA1881
CHA1882
CHA1883
CHA1884
CHA1885
CHA1886
CHA1887
CHA1888
CHA1889
CHA1890
CHA1891
CHA1892
CHA1893
CHA1894
CHA1895
CHA1896
CHA1897
CHA1898
CHA1899
CHA1900
CHA1901
CHA1902
CHA1903
CHA1904
CHA1905
CHA1906
CHA1907
CHA1908
CHA1909
CHA1910
CHA1911
CHA1912
CHA1913
CHA1914
CHA1915
CHA1916
CHA1917
CHA1918
CHA1919
CHA1920
CHA1921
CHA1922
CHA1923
CHA1924
CHA1925
CHA1926
CHA1927
CHA1928
CHA1929
CHA1930
CHA1931
CHA1932
CHA1933
CHA1934
CHA1935
CHA1936
CHA1937
CHA1938
CHA1939
CHA1940
CHA1941
CHA1942
CHA1943
CHA1944
CHA1945
CHA1946
CHA1947

	FIDOT4=-ROU00*DFDXI4+DFIDT4	CHA1948
	UXDOT=-ROU00*DUDXIX+DUDTX	CHA1949
	PXDOT=-ROU00*DPDXIX+DPDXTX	CHA1950
	ROXDOT=-ROU00*DRDXIX+DRODTX	CHA1951
	ZXDOT=-ROU00*DZDXIX+DZDXTX	CHA1952
	FIH1=FI1+DT2*FIDOT1	CHA1953
	FIH2=FI2+DT2*FIDOT2	CHA1954
	GIH=PX+DT2*PXDOT	CHA1955
	FIH3=FI3+DT2*FIDOT3	CHA1956
	FIH4=FI4+DT2*FIDOT4	CHA1957
	UXN=UX+DT*UXDOT	CHA1958
	PXN=PX+DT*PXDOT	CHA1959
	ROXN=ROX+DT*ROXDOT	CHA1960
	ZXN=ZX+DT*ZXDOT	CHA1961
	IF(ZXN.LT.0.) ZXN=0.	CHA1962
	GO TO 90	CHA1963
20	CONTINUE	CHA1964
	EVO=GL*DSQRT(BETA0)	CHA1965
201	CONTINUE	CHA1966
	DFIDA1=DRODAX*UX+ROX*DUDAX	CHA1967
	DFIDA2=DRODAX*UX**2+2.D0*ROX*UX*DUDAX+DPDAX	CHA1968
	DFIDA2=DFIDA2-DPDAX	CHA1969
	DFIDA3=DUDAX*(G12*PX+0.5D0*ROX*UX**2)	CHA1970
1	+UX*(G12*DPDAX+0.5D0*DRODAX*UX**2+ROX*UX*DUDAX)	CHA1971
	DFIDA4=ZX*DFIDA1+ROX*UX*DZDAX	CHA1972
	FIDOT1=-EVO*DFIDA1	CHA1973
	FIDOT2=-EVO*DFIDA2	CHA1974
	FIDOT3=-EVO*DFIDA3	CHA1975
	FIDOT4=-EVO*DFIDA4	CHA1976
	FIH1=FI1+DT2*FIDOT1	CHA1977
	FIH2=FI2+DT2*FIDOT2	CHA1978
	FIH3=FI3+DT2*FIDOT3	CHA1979
	FIH4=FI4+DT2*FIDOT4	CHA1980
	GA=DGDAX	CHA1981
	IF(NFLUX.EQ.5)GA=-GA	CHA1982
	DROUA=UX*DRODAX+ROX*DUDAX	CHA1983
	BETAPR=0.5D0*DSQRT(BETA0)*(GA-DROUA)	CHA1984
	FIH2=FIH2-DPDBX*BETAPR*DT2	CHA1985
	UXDOT=-EVO*DUDAX+BETAPR*DUDBX	CHA1986
	PXDOT=-EVO*DPDAX+BETAPR*DPDBX	CHA1987
	GIH=PX+DT2*PXDOT	CHA1988
	ROXDOT=-EVO*DRODAX+BETAPR*DRODBX	CHA1989
	ZXDOT=-EVO*DZDAX	CHA1990
	UXN=UX+DT*UXDOT	CHA1991
	PXN=PX+DT*PXDOT	CHA1992
	ROXN=ROX+DT*ROXDOT	CHA1993
	ZXN=ZX+DT*ROXDOT	CHA1994
	IF(ZXN.LT.0.) ZXN=0.	CHA1995
	GO TO 90	CHA1996
50	CONTINUE	CHA1997
	EVO=-GR*DSQRT(BETA0)	CHA1998
	GO TO 201	CHA1999
30	CONTINUE	CHA2000
40	CONTINUE	CHA2001
	GO TO 60	CHA2002
90	CONTINUE	CHA2003
	RETURN	CHA2004
	END	CHA2005

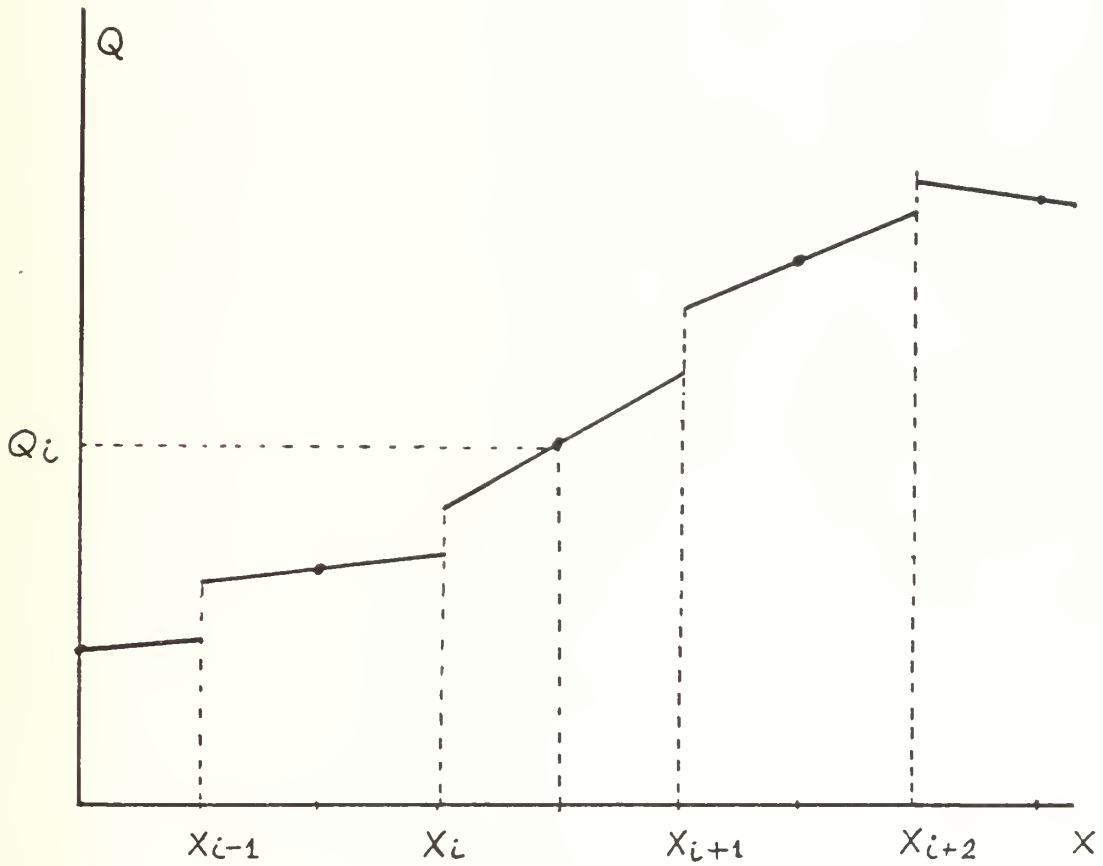


Figure A-1. Piecewise Linear Distribution of Flow Variables in Cells

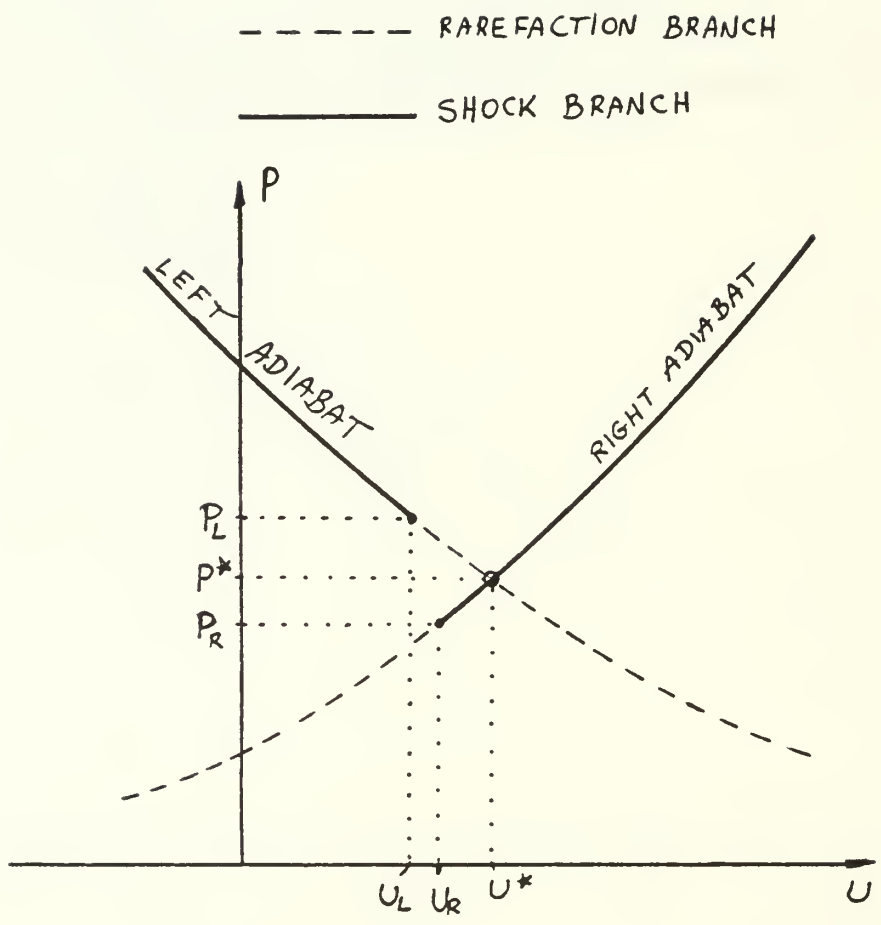


Figure A-2. Intersection of Right and Left Adiabats for Solving Riemann Problem

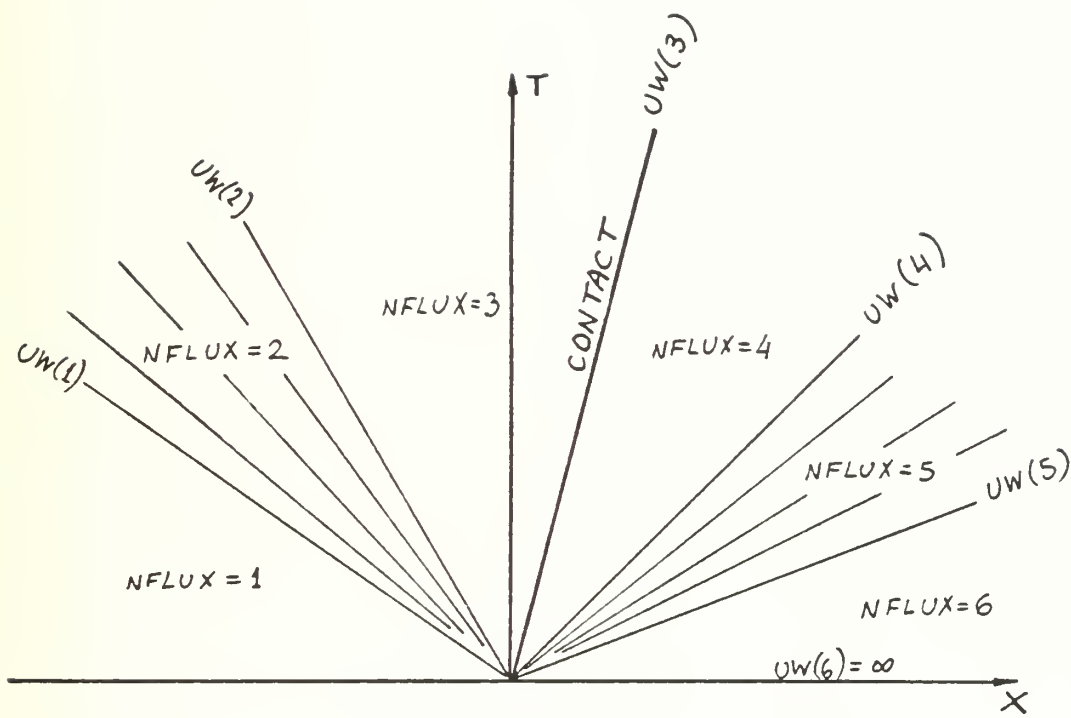


Figure A-3. Wave Diagram Representing Solution to Riemann Problem

APPENDIX B. Code for Re-Normalizing the Air Impulse

```

1      IMPLICIT REAL*8(A-H,O-Z)
C      CODE RENORM -- C TRANSFORMATION OF TOTAL REFLECTED IMPULSE FROM
C      BAKER'S CHART TO SPACE-NORMALIZED VALUES.
C      DATA FROM FIG. 6.3 (SUPPLEMENT) IN BAKER'S BOOK "EXPLOSIONS IN AIR"
2      REAL*4 RB,IB,RS,IS,ISBARE
3      DIMENSION RB(21),IB(21)
4      DIMENSION RS(21),IS(21),ISBARE(21)
5      DATA RB/.05,.06,.07,.08,.09,.1,.2,.3,.4,.5,.6,.7,.8,.9,1.,
1      2.,3.,4.,5.,6.,7./
6      DATA IB/4.4,3.06,2.30,1.83,1.50,1.27,.457,.293,.221,.178,.149,
1      .128,.113,.099,.0885,.0376,.0236,.0173,.0136,.0113,.0095/
7      PAI=4.D0*DATAN(1.D0)
8      G=1.4D0
9      PA=0.1D0
10     RHOA=1.3D0
11     RHOO=1800.D0
12     QO=4.D0
13     BETA=DSQRT(RHOA/RHOO)*(PA/(RHOO*QO))**(1.D0/6.D0)
14     GOREM=(3.D0/DSQRT(2.D0*G))**(4.D0*PAI/3.D0))**(1.D0/3.D0)
15     BETA=BETA*GOREM
16     DELTA=( (4.D0*PAI/3.D0)*(RHOO*QO/PA) )***(1.D0/3.D0)
17     PRINT 11, BETA,DELTA
18 11  FORMAT(/1X,'RESULTS WITH BETA,DELTA=',2D16.7//
1      1X,' N',' RB ',' IB ',' 2X,
2      ' RS ',' IS ',' ISBARE '/')
19     DO 1 N=1,21
20     RS(N)=RB(N)*DELTA
21     IS(N)=IB(N)*BETA
22     ISBARE(N)=1.D0/RS(N)**2
23     PRINT 2, N,RB(N),IB(N),RS(N),IS(N),ISBARE(N)
24 2   FORMAT(1X,I4,2E12.4,2X,2E12.4,2X,E12.4)
25 1   CONTINUE
26     END

```

RESULTS WITH BETA,DELTA= 0.1204163D-01 0.6706157D+02

N	RB	IB	RS	IS	ISBARE
1	0.5000E-01	0.4400E+01	0.3353E+01	0.5298E-01	0.8894E-01
2	0.6000E-01	0.3060E+01	0.4024E+01	0.3685E-01	0.6177E-01
3	0.7000E-01	0.2300E+01	0.4694E+01	0.2770E-01	0.4538E-01
4	0.8000E-01	0.1830E+01	0.5365E+01	0.2204E-01	0.3474E-01
5	0.9000E-01	0.1500E+01	0.6036E+01	0.1806E-01	0.2745E-01
6	0.1000E+00	0.1270E+01	0.6706E+01	0.1529E-01	0.2224E-01
7	0.2000E+00	0.4570E+00	0.1341E+02	0.5503E-02	0.5559E-02
8	0.3000E+00	0.2930E+00	0.2012E+02	0.3528E-02	0.2471E-02
9	0.4000E+00	0.2210E+00	0.2682E+02	0.2661E-02	0.1390E-02
10	0.5000E+00	0.1780E+00	0.3353E+02	0.2143E-02	0.8894E-03
11	0.6000E+00	0.1490E+00	0.4024E+02	0.1794E-02	0.6177E-03
12	0.7000E+00	0.1280E+00	0.4694E+02	0.1541E-02	0.4538E-03
13	0.8000E+00	0.1130E+00	0.5365E+02	0.1361E-02	0.3474E-03
14	0.9000E+00	0.9900E-01	0.6036E+02	0.1192E-02	0.2745E-03
15	0.1000E+01	0.8850E-01	0.6706E+02	0.1066E-02	0.2224E-03
16	0.2000E+01	0.3760E-01	0.1341E+03	0.4528E-03	0.5559E-04
17	0.3000E+01	0.2360E-01	0.2012E+03	0.2842E-03	0.2471E-04
18	0.4000E+01	0.1730E-01	0.2682E+03	0.2083E-03	0.1390E-04
19	0.5000E+01	0.1360E-01	0.3353E+03	0.1638E-03	0.8894E-05
20	0.6000E+01	0.1130E-01	0.4024E+03	0.1361E-03	0.6177E-05
21	0.7000E+01	0.9500E-02	0.4694E+03	0.1144E-03	0.4538E-05

6. DISTRIBUTION LIST	No. of Copies
1. Defense Technical Information Center Cameron Station Alexandria, VA 22314	2
2. Library, Code 0142 Naval Postgraduate School Monterey, CA 93943-5100.	2
3. Department Chairman, Code 67 Department of Aeronautics Naval Postgraduate School Monterey, CA 93943-5100.	1
4. Distinguished Professor Allen E. Fuhs Space Systems Academic Group, Code 72 Naval Postgraduate School Monterey, CA 93943-5100.	5
5. Dr. Neil Griff SDIO/DEO Washington, DC 20301-7100.	3
6. Mr. Bruce Pierce SDIO/DEO Washington, DC 20301-7100.	1
7. Dr. Joseph Falcovitz Code 72 Naval Postgraduate School Monterey, CA 93943-5100.	5

- 8. Professor R. E. Ball
 Department of Aeronautics, Code 67
 Naval Postgraduate School
 Monterey, CA 93943-5100. 1

- 9. Professor Y. S. Shin
 Department of Mechanical Engineering, Code 69
 Naval Postgraduate School
 Monterey, CA 93943-5100. 1

- 10. Research Administration Office
 Code 012
 Naval Postgraduate School
 Monterey, CA 93943-5100. 1

- 11. Dr. P. Avizonis
 Air Force Weapons Laboratory
 Kirtland Air Force Base, NM 87117 1

- 12. Dr. John Lawless
 Space Power Inc.
 1977 Concourse Drive
 San Jose, CA 95131 1

- 13. Dr. Mark Thornton
 Boeing Aerospace Company
 Post Office Box 3999
 Seattle, WA 98124-2499 1

- 14. LT. Mark Price
 AFRPL
 Edwards AFB, CA 93523 1

- 15. Mr. Arthur W. Rogers
Space Systems Division
Hughes Aircraft Co.
P. O. Box 92919, Los Angeles, CA 90009 1

- 16. LCOL Rick Babcock, USAF
Air Force Geophysical Laboratory
Hanscomb Field
Bedford, MA 01730 1

DUDLEY KNOX LIBRARY



3 2768 00336622 0